# Efficient CRISPR/Cas12a-based genome editing toolbox for metabolic engineering in *Methanococcus maripaludis*

Authors: Jichen Bao, Enrique de Dios Mateos, Silvan Scheller*

Department of Bioproducts and Biosystems, School of Chemical Engineering, Aalto University, FI-02150, Espoo, Finland

*corresponding author: Silvan Scheller (silvan.scheller@aalto.fi)

Tel: +358 50 3565 175

ORCID

Silvan Scheller 0000-0002-0667-9224

Jichen Bao 0000-0002-5959-2640

**ABSTRACT:**

The rapid-growing and genetically tractable methanogen *Methanococcus maripaludis* is a promising host organism for the biotechnological conversion of carbon dioxide and renewable hydrogen to fuels and value-added products. Expansion of its product scope through metabolic engineering necessitates reliable and efficient genetic tools, particularly for genome edits to the primary metabolism that affect cell growth. Here, we have designed a genome editing toolbox by utilizing Cas12a from *Lachnospiraceae bacterium* ND2006 (LbCas12a) in combination with the homology-directed repair machinery endogenously present in *M. maripaludis*. Remarkably, this toolbox can knock out target genes with a success rate of up to 95%, despite the hyper-polyploidy of *M. maripaludis*. For the purposes of demonstrating a large-sized deletion, we have replaced the flagellum operon (ca. 8.9 kbp) by the β-glucuronidase gene. To facilitate metabolic engineering and flux balancing in *M. maripaludis*, the relative strength of 15 different promoters were quantified in the presence of the two common growth substrates, formate or carbon dioxide and hydrogen. This CRISPR/LbCas12a toolbox can be regarded as a reliable and fast method for genome editing in a methanogen.

**Keywords:** *Methanococcus maripaludis*, methanogens, CRISPR/Cas12a, genome editing, metabolic engineering, synthetic biology

37 **INTRODUCTION**

38 Methanogenic archaea are biotechnologically employed in a variety of uses, e.g. for methane
39 production in anaerobic digestors[1], as biocatalysts in power-to-gas processes[2], and as promising host
40 organisms for synthetic pathways to convert carbon dioxide ($CO_2$) into value-added products[3,4].
41 Hydrogenotrophic methanogens utilize the reductive acetyl-CoA pathway for $CO_2$ fixation[5], an
42 energy-efficient route to synthesize organic carbon from $CO_2$ and hydrogen ($H_2$), which is similar to
43 that found in acetogens[6]. However, subtle differences exist between the acetogenic[7] and
44 methanogenic pathways of $CO_2$ reduction in terms of ATP investment and cofactor utilization[8].
45 Depending on the requested product that needs to be generated from $CO_2$ as the carbon source,
46 methanogens may be better suited host organisms than acetogens. Recently, the methanogen
47 *Methanosarcina acetivorans* was re-engineered to no longer depend on methane production for its
48 energy metabolism[9], and thereby it might serve as an example where a methanogen could be
49 utilized for generating an increased repertoire of new potential products, besides just methane.

50 *Methanococcus maripaludis* is a promising methanogenic host organism for metabolic engineering
51 of $CO_2$-fixation pathways due to its advantageous growth properties, e.g., two-hour doubling
52 time[10,11], moderate growth temperature of 38°C, and ability to fix nitrogen[12,13,14]. Typical electron
53 donors for $CO_2$ reduction in *M. maripaludis* include formate, $H_2$, and bioelectrically coupled
54 systems[15,16]. Efforts to expand the product scope beyond methane for *M. maripaludis* are already
55 underway. As an example, the mevalonate pathway in this methanogen was metabolically
56 engineered to produce geraniol from $CO_2$ and formate[4]. Even so, efficient and reliable genome
57 editing tools are critical for successful metabolic engineering in *M. maripaludis*. Marker recycling is
58 prerequisite for multi target engineering. In the case of *M. maripaludis*, although a 'pop-in/pop-out'
59 markerless-based genome editing technique has been developed[17], it tends to have a problematic
60 low positive rate, which can sometimes be less than 5%[17], especially for those modifications that
61 affect cell growth. As an alternative, the CRISPR/Cas (clustered regularly interspaced short
62 palindromic repeats/CRISPR associated protein) system might remedy this problem because of its
63 reputation for highly efficient genome editing.

64 The CRISPR/Cas9 system has already been successfully used for genome editing in a variety of
65 organisms[18,19,20,21,22,23] owing to its simplicity and high efficiency. However, only a few CRISPR
66 genome editing toolboxes have been developed for archaea[24]. The first CRISPR/Cas9-mediated
67 genome editing system for a methanogen was reported in 2017 using *M. acetivorans* as the model
68 organism[25]. This Cas9-based system recognizes and cleaves a 20 nt target sequence that is flanked by
69 a 3′-NGG protospacer adjacent motif (PAM). This contrasts with Cas12a, which instead recognizes
70 the 5′-thymine (T)-rich PAM 5'-TTTV. This recognition site makes Cas12a the better option for
71 developing a CRISPR toolbox in microbes with an adenine (A)- and T-rich genome. Another
72 advantageous attribute of Cas12a lies in its ribonuclease activity, which allows the formation of
73 multiple guide RNAs (gRNAs) from a single transcript[26,27]. Since the *M. maripaludis* genome has a
74 high AT content (67.1%), we decided to use the Cas12a from *Lachnospiraceae bacterium* ND2006
75 (LbCas12a) and combine it with the intrinsic homology-directed repair machinery to develop a
76 CRISPR genome editing toolbox. In our study, we examined how the length of the repair fragment
77 (RF) and the distance of the RF to the double stranded break (DSB) can impact on the genome-
78 editing efficiency. To further expand the versatility and editing potential of this genetic toolbox, we
79 also established a Cas9-based editing system. As an application of our toolbox, we deleted the *M.*
80 *maripaludis* flagellum operon and replaced it by the β-glucuronidase gene. Finally, we were also able
81 to quantify the relative strength of 15 different *M. maripaludis* promoters in the presence of the two
82 common growth substrates formate or $H_2$+$CO_2$.

83

84 **RESULTS AND DISCUSSION**

85 **CRISPR/Cas12a-based introduction of double-stranded breaks and transformation efficiency.** The
86 host strain *M. maripaludis* JJΔupt was used for all experiments, applying the natural transformation
87 protocol recently established[28]. The *Escherichia coli*/*M. maripaludis* shuttle vector pLW40[29] was used
88 as a backbone to construct the final toolbox plasmid pMM002P (Table 1). The schematic diagram of
89 the toolbox plasmid and description of its components is given in Fig.1a. The transformation
90 efficiency of pMM002P in JJΔupt was ca. 5 x $10^4$ colony forming units per 2 $\mu$g DNA [cfu (2 $\mu$g DNA)$^{-}$
91 $^{1}$](Fig. 1b), which is higher than the reported efficiency of the empty plasmid pLW40neo [2.4 x $10^3$
92 cfu (2 $\mu$g DNA)$^{-1}$][28]. The high transformation efficiency indicates that expressing LbCas12a alone is
93 not toxic to the host cell. When one gRNA was co-expressed with LbCas12a, only 3-18 colonies could
94 be observed on the transformation plates. When two gRNAs were co-expressed, only 0-3 colonies
95 were formed (Fig. 1b). These results indicated that the LbCas12a-gRNA complex can perform a lethal
96 double stranded break in *M. maripaludis*. Nonhomologous end joining (NHEJ) machineries are rare in
97 archaea[30], and we could not find the homologous Ku protein in *M. maripaludis* JJ. Thus, the NHEJ
98 does not cause the escape from the cleavage.

99

100 **Genome editing via CRISPR/LbCas12a by providing a repair fragment on the same plasmid.** A gRNA
101 was expressed on pMM002P (p002-218) targeted to the gene *flaI* within the flagellum operon. The
102 lethal effect of the functional gRNA could be relieved by including RFs with various lengths of the
103 homology arms (Fig. 2a). When a 1000 bp long homologous arm on each side was provided, the
104 transformation efficiency reached 2.8 x $10^4$ cfu (2 $\mu$g DNA$^{-1}$). We therefore used the 1000 bp long
105 homologous arms as the standard condition in the following experiments. 250 bp long homologous
106 arms would be enough to rescue the DSB generated by Cas12a/gRNA complex, but the
107 transformation efficiency is 70 times lower.

108 The influence of the distance between the RF and the DSB on the transformation efficiency has been
109 tested by utilizing ~25, ~500, and ~1000 bp distances (Fig. 2b). At ~500 bp distance, the
110 transformation efficiency was 5 times lower than at ~25 bp (two sided *t*-test, $p < 0.001$), but there
111 was no significant difference between ~500 and ~1000 bp distance (two sided *t*-test, $p > 0.05$).
112 Because the *M. maripaludis* JJ strain has an intrinsic *Pst* I restriction/modification system, the host
113 cells can digest the foreign DNA containing unmethylated *Pst* I sites, and one *Pst* I site may cause a
114 1.6 - 3.4 fold decrease in transformation efficiency[31]. There is one *Pst* I site on the homologous arm
115 on both plasmids (500 bp and 1000 bp), resulting in a lower number of transformants (Fig. 2b). Since
116 the transformation efficiency is the same in the experiments with ~500 bp and with ~1000 bp
117 distances to the DSB, we conclude that the editing efficiency is not significantly affected up to 1000
118 bp distances.

119 To test the positive rate, a pair of primers were used to amplify the up- and down-stream of the
120 homologous arms on the chromosome. The PCR products were further digested by the
121 endonuclease NotI. The NotI restriction site was pre-designed between the left and the right RF in
122 order to distinguish the wildtype copies and the edited ones (Fig. S1-S3). The system enabled 89 -
123 100% positive rate of genome editing (Fig. 2a, Fig. S1-S5). The results indicate that the
124 CRISPR/Cas12a toolbox performs reliable genome editing in *M. maripaludis*. Combining all
125 experiments presented in Fig. 2, 63/66 colonies were correctly edited, which corresponds to an
126 average positive rate of ca. 95%.

127

128 **Genome editing via CRISPR/LbCas12a by providing a repair fragment separately.** As a variant of the
129 optimized method described above, we have provided the RF as a suicide plasmid which may speed
130 up the work for creating different mutants in parallel. In the section "Quantification of promoter
131 strengths" below, the tested promoters did drive the expression of *uidA* via a "*Promoter-uidA*"
132 expression cassette that has been integrated onto the locus of acetyl-CoA synthetase (MMJJ_09370)
133 via co-transforming the CRISPR/LbCas12 cleavage plasmid with a suicide plasmid containing
134 "*Promoter-uidA*" cassette flanked by 1 kbp up- and down-stream homologous arms. We obtained
135 transformants for this variation with the suicide plasmid, but the transformation efficiency was ca.
136 10 - 50 fold lower. Although the transformation efficiency is lower in this variant of the standard
137 toolbox, the positive rate appears not to be affected. For all 15 different constructs with suicide
138 plasmid, we randomly tested 3 transformants of each construct, 45/45 of the colonies were found to
139 be positive (Fig. S8)

140 An additional possibility is to co-transform the CRISPR/LbCas12a cleavage plasmid with a separate RF
141 that was provided as a PCR fragment. Genome editing was successful, but the efficiency was ca. 100-
142 1000 times lower compared to our optimized method with the full p002-g218-L1000 plasmid.

143

144 **Replacing a large genome fragment by a heterologous gene via the CRISPR/Cas12a toolbox.** To
145 apply the toolbox for the heterologous gene integration, we have replaced the whole flagellum
146 operon (*flaB1B2B3CDEFGHIJ*, length 8.9 kbp) by *uidA* from *E. coli* that codes for a β-glucuronidase.
147 We carried out two different procedures: A) Using one gRNA that generates one lethal DSB on the
148 chromosome, resulting in two long distances from DSB to the repair fragment of 6.4 and 2.5 kbp. B)
149 Cutting on both sides of the *fla* operon by using two different gRNAs, which shortens the distances
150 from DSB to the repair fragment to 0.25 kbp and 3.2 kbp. Both procedures were successful with a
151 similar transformation efficiency (Fig. 3), showing that our toolbox is able to make a large fragment
152 deletion in the genome. The positive rate was lower in procedure A, where one distance was 6.4 kbp
153 (Fig. 3, Fig. S6 and S7), implying that the positive rate is affected when the distance is substantially
154 longer than 1000 bp. A similar observation has been reported for *M. acetivorans*: There, the positive
155 rate dropped significantly when the distance to the DSB was larger than 1000 bp[25], and the
156 transformation efficiency decreased with increasing distance[25]. Deleting a large fragment by using
157 two gRNAs in order to shorten the distance from RF to DSB demonstrated here may therefore also
158 improve the transformation efficiency and positive rate in other CRISPR systems for methanogenic
159 hosts.

160

161 **Genome editing via CRISPR/SpCas9.** To expand the versatility and number of usable gRNAs of the
162 CRISPR toolbox, we also constructed a Cas9-based editing plasmid, based on Cas9 from
163 *Streptococcus pyogenes*. To test this additional tool, the gene coding for the alanine dehydrogenase
164 – alanine racemase was successfully replaced by a 4.2 kbp fragment via co-transforming a
165 CRISPR/SpCas9 plasmid with a gRNA and a suicide plasmid containing the 4.2 kbp fragment flanked
166 by 1000 bp up- and down-stream homologous arms. The transformation efficiency was 317 ± 123
167 cfu (2 $\mu$g DNA)$^{-1}$ and the positive rate was 8/10 (Fig. S9, Fig. S10). There were two *Pst* I sites on the
168 repair fragment, which can explain the lower transformation efficiency.

169

170 **Quantification of promoter strengths.** We have tested 15 different promoters: 12 from the closely
171 related methanogen *Methanococcus vannielii* SB, and the three native promoters $P_{mcr}$, $P_{mcr}$ reverse
172 ($P_{mcrR}$) and $P_{fla}$. The promotors strengths have been quantified under the two common growth
173 conditions formate or $H_2$+$CO_2$. All promoters could drive the expression of *uidA* under both growth
174 conditions (formate or $H_2$+$CO_2$ as substrate), except $P_{nif}$ and $P_{hdrC1}$ (Fig. 4). The promotor $P_{hdrC1}$
175 allowed gene expression in formate medium, but not in $H_2$+$CO_2$ medium. The $P_{mcr}$ promoter is
176 considered as a strong constitutive promoter in methanogens [32]. Therefore, $P_{glnA}$, $P_{mtr}$, $P_{mcr}$, $P_{mcr_JJ}$,
177 $P_{fla_JJ}$ can be classified as strong promoters in *M. maripaludis*. The $P_{nif}$ promoter is repressed by the
178 nitrogen regulator, NrpR, and the $P_{nif}$ becomes highly active once $N_2$ is used as a sole nitrogen source
179 or the transcription repressor NrpR is absent[33]. We have deleted *nrpR* in the "$P_{nif}$-*uidA*" strain and
180 found that the strength of $P_{nif}$ increased significantly (2670 ± 58 nmol $min^{-1}$ $OD_{600}^{-1}$) (two sided *t*-test,
181 $P < 0.001$) when NrpR was absent in *M. maripaludis*. Thus, the "Δ*nrpR*-$P_{nif}$" expression may be used
182 for target genes requiring a very strong expression.

183 The majority of the tested promoters had a similar strength on both growth-conditions, formate and
184 $H_2$+$CO_2$. The $P_{eha}$ promoter that drives the expression of the energy conservating hydrogenase A,
185 *eha*, in *M. vannielii* was weak in *M. maripaludis*. Notably, the $P_{eha}$ did not directly express the
186 subunits of *eha*. The first gene driven by $P_{eha}$ is a putative transcription regulator. Thus, we also tried
187 to express *uidA* after the the putative transcription regulator ($P_{eha\ w.TF}$). The expression level of UidA
188 was significantly higher with $P_{eha\ w.TF}$ than $P_{eha}$ (two sided *t*-test, $p < 0.01$) in both growth conditions.
189 These results imply that the transcription regulator might be involved in the regulation of *eha*.

190 The $P_{glnA}$ promoter from *M. vannielii* was unexpectedly strong in *M. maripaludis* despite of the
191 presence of NrpR and ammonium in the medium. In order to exclude a potential mutation, we have
192 sequenced the $P_{glnA}$-*uidA* expression cassette from the genome of the engineered *M. maripaludis*
193 strain, but no mutation could be found. We have also repeated the transformation and re-picked
194 several different transformants to test the UidA activity. All transformants showed a high expression
195 level of UidA. Thus, we can conclude that $P_{glnA}$ from *M. vannielii* is a strong promoter in *M.*
196 *maripaludis*. The native $P_{glnA}$ promoter has a basal constitutive expression level in *M. maripaludis*
197 when ammonium is present[34]. Although the *glnA* operator from $P_{glnA}$ promoter is the same as the
198 one from *M. maripaludis*, the expression level of "$P_{glnA}$ -*uidA*" appears to be the highest among all
199 promoters tested.

200

201 **CONCLUSION**

202 *M. maripaludis* already has genetic tools and efficient transformation protocols[17,31,28] for standard
203 applications, but many colonies may need to be screened to obtain the desired genotype by the
204 classic pop-in-pop-out genome editing technique[17], especially when the targets to be engineered
205 affect cell growth[32]. As a solution, we have established a reliable CRISPR/Cas12a toolbox in *M.*
206 *maripaludis* for gene knock-in and knock-out with positive rate of ca. 95%. Our system only requires
207 one round of homologous recombination, and no merodiploid is formed, which lowers the workload
208 of genome editing and increases the success rate. The option of providing the repair fragment
209 separately as a suicide plasmid or as a PCR template may further speed up the editing progress.
210 Since Cas12a has intrinsic ribonuclease activity that can process multiplex gRNA in one transcript
211 without extra ribonuclease[26,27], it can be convenient to express two gRNAs via the CRISPR/LbCas12a
212 system, saving time and cost of plasmid construction.

213 Proteins can be expressed heterologously in *M. maripaludis* via stable integration of the
214 corresponding genes. Utilizing *M. maripaludis* as an expression host may be advantageous for
215 proteins that are difficult to be expressed in *E. coli*, such as formate dehydrogenases[16], methyl-
216 coenzyme M reductases[35], or heterodisulfide reductases[36].

217 Although different promoters have already been studied and used for synthetic biology in *M.*
218 *maripaludis*[37,14,38,33], there has not been a uniform system to compare their strengths, which is now
219 available and allows to balance metabolic fluxes in engineered *M. maripaludis* strains.

220

221 **MATERIALS AND METHODS**

222 **Strain and plasmids.** All plasmids and strains used in this study are listed in Table S1 and Table S2.
223 The links of plasmid maps are listed in Table S3. *M. maripaludis* JJΔupt[28] and plasmid pLW40[29] are
224 gifts from Prof. Kyle Costa, University of Minnesota. Plasmid pMEV4[4] was kindly provided by Prof.
225 William B Whitman, University of Georgia. *M. maripaludis* S2[39] was kindly provided by Prof. John
226 Leigh and Dr. Thomas Lie, University of Washington. NEB5α (New England Biolabs) was used for
227 plasmid construction. The plasmid pMM002P and pMM005 was constructed by Gibson assembly[40].
228 The construction procedure and primers of pMM002P and pMM005 are described in Table S4 and
229 S5. All the cleavage plasmids were constructed as follows: (1) for LbCas12a gRNA, the forward
230 primer was designed as "5'-AGAT+(23nt guide sequence)", the reverse primer was designed as "5'-
231 TATC+(23nt reverse complement guide sequence)"; for SpCas9 gRNA, the forward primer was
232 designed as "5'-AGTG+(20nt guide sequence)", the reverse primer was designed as "5'- AAAC+(20nt
233 reverse complement guide sequence) (2) the two primers which contain the gRNA and have 4 nt
234 overhang at 5'-end were annealed (3) the annealing product was ligated with *PaqC* I (New England
235 Biolabs)-digested pMM002P or pMM005. The guide sequences was designed on CHOPCHOP
236 (https://chopchop.cbu.uib.no/)[41]. The RF was inserted into the corresponding cleavage plasmid at
237 the *Mre* I restriction site. The rest primers used in this study are listed in Table S6.

238

239 **Medium and cultivation conditions.** Luria–Bertani medium with 50 mg $L^{-1}$ ampicillin was used for
240 plasmid construction and amplification. McC medium was used for *M. maripaludis* strain cultivation
241 with 2.8 bar 80% $H_2$/20% $CO_2$ in the headspace[28]. The culture tubes were incubated at 37°C at 200
242 rpm. McFC medium was used when formate was used as a carbon source[42] The culture tubes were
243 incubated at 37°C without shaking. 2.5 $\mu$g $mL^{-1}$ puromycin or 0.25 mg $mL^{-1}$ 6-azauracil was added
244 where required.

245

246 ***M. maripaludis* transformation.** The natural transformation protocol was used as previously
247 described[28]. Briefly, 5 mL of *M. maripaludis* culture was grown overnight to an $OD_{600}$ between 0.7
248 and 1.2. 2 $\mu$g of DNA was added into the culture directly, followed by flushing the headspace with
249 80% $H_2$/20% $CO_2$; for 0.5 min and pressurizing the cultivation to 2.8 bar. The tube was then
250 incubated in a shaker at 37°C at 200 rpm for 4 h and the cells plated on McC medium.

251

252 **Removal of the CRISPR/Cas plasmid.** The *M. maripaludis* strains containing the CRISPR/Cas toolbox
253 plasmid was grown in 5 mL of McC medium without antibiotics to an $OD_{600}$ between 0.7 and 1.2.
254 Then 100 $\mu$L of the preculture was inoculated in another 5 mL of McC medium without antibiotics

for overnight. On the next day, one drop of culture was streaked on the McC medium with 6-azauracil plate. After 3-5 days, several individual colonies were picked and streaked on another McC medium 6-azauracil plate for purification.

**β-glucuronidase activity measurements.** 4-Nitrophenyl β-*D*-glucuronide (4-NPG, CAS no. 10344-94-2) (Sigma-aldrich) was prepared in 50 mM sodium phosphate buffer (Na-PB) (pH=7.0) as a stock solution (10 mg $mL^{-1}$). The detailed procedure was as follows: the cells were grown to an $OD_{600}$ of ca 0.5; the exact $OD_{600}$ was measured (BioPhotometer plus, Eppendorf); 1 mL of cell culture was pelleted via centrifugation; the cell pellet was resuspended in 500 $\mu$L of Na-PB; around 30 µl glass beads were added; the tube was vortexed for 5 min to break the cells thoroughly; the tube was centrifuged and the supernatant collected; the sample was diluted to 500 $\mu$L in Na-PB; the sample incubated at 37°C for 20 minutes; 40 $\mu$L 4-NPG was added; reaction mixture was kept at 37°C for 15 minutes to react; 400 $\mu$L 200 mM $Na_2CO_3$ was added to stop the reaction; the absorbance at 405 nm was read. The specific activities have been calculated using β-glucuronidase from *E. coli* K12 (Product no. 3707580001, Sigma-Aldrich) as the standard, using the conversion factor of 398 nmol $min^{-1}$. The standard curve is shown in Fig. S11.

## AUTHOR CONTRIBUTIONS

JB and SS conceived the study and wrote the manuscript. JB and EDM performed the experiments. All authors commented and approved the final version of the manuscript. All authors declare no conflict of interest.

## ACKNOWLEDGEMENTS

We thank the summer-students Han Le, An Nguyen and Pradhuman Jetha for contributing to the plasmid construction work and *M. maripaludis* transformation. We thank Prof. Kyle Costa for providing strain JJΔupt and plasmid pLW40, Prof. William B. Whitman for providing plasmid pMEV4,pMEV4mTs, and strain *M. voltae* A3, and Prof. John Leigh and Dr. Thomas Lie for providing strain S2. Prof. Michael Rother, Prof. Qunxin She and Prof. Dipti Nayak are acknowledged for helpful discussions. We thank Dr. Norman Adlung, Dr. Ingemar von Ossowski and Dr. Vera Jäger for the critical comments on the manuscript. We thank the Novo Nordisk Foundation for funding (grant NNF19OC0054329 to S. S.).

287 **REFERENCES**


288 (1) Wintsche, B.; Jehmlich, N.; Popp, D.; Harms, H.; Kleinsteuber, S. Metabolic adaptation of
289 methanogens in anaerobic digesters upon trace element limitation. *Front. Microbiol.* **2018**, *9*,
290 1–10. https://doi.org/10.3389/fmicb.2018.00405.

291 (2) Braga Nan, L.; Trably, E.; Santa-Catalina, G.; Bernet, N.; Delgenès, J. P.; Escudié, R.
292 Biomethanation processes: new insights on the effect of a high $H_2$ partial pressure on
293 microbial communities. *Biotechnol. Biofuels* **2020**, *13* (1), 1–17.
294 https://doi.org/10.1186/s13068-020-01776-y.

295 (3) Aldridge, J.; Carr, S. Anaerobic production of isoprene by engineered *Methanosarcina* species.
296 *Archaea*. **2021**, *87* (6), 1–14.

297 (4) Lyu, Z.; Jain, R.; Smith, P.; Fetchko, T.; Yan, Y.; Whitman, W. B. Engineering the autotroph
298 Methanococcus maripaludis for geraniol production. *ACS Synth. Biol.* **2016**, *5* (7), 577–581.
299 https://doi.org/10.1021/acssynbio.5b00267.

300 (5) Peter G. Simpson; Whitman, W. B. Anabolic pathways in methanogens. In *Methanogenesis*;
301 Springer, Boston, MA: Chapman & Hall, New York, 1993; pp 445–472.
302 https://doi.org/https://doi.org/10.1007/978-1-4615-2391-8_11.

303 (6) Ragsdale, S. W.; Pierce, E. Acetogenesis and the Wood-Ljungdahl pathway of $CO_2$ fixation.
304 *Biochim. Biophys. Acta - Proteins Proteomics* **2008**, *1784* (12), 1873–1898.
305 https://doi.org/10.1016/j.bbapap.2008.08.012.

306 (7) Müller, V. New Horizons in acetogenic conversion of one-carbon substrates and biological
307 hydrogen storage. *Trends Biotechnol.* **2019**, 1–11.
308 https://doi.org/10.1016/j.tibtech.2019.05.008.

309 (8) Lemaire, O. N.; Jespersen, M.; Wagner, T.; Scott, K. $CO_2$ -fixation strategies in energy
310 extremophiles: what can we learn from acetogens? *Front. Microbiol*. **2020**, *11*, 1–8.
311 https://doi.org/10.3389/fmicb.2020.00486.

312 (9) Schone, C.; Poehlein, A.; Jehmlich, N.; Adlung, N.; Daniel, R.; von Bergen, M.; Scheller, S.;
313 Rother, M. Deconstructing *Methanosarcina acetivorans* into an acetogenic archaeon. *Proc.*
314 *Natl. Acad. Sci. U. S. A.* **2022**, *119* (2), 1–7. https://doi.org/10.1073/pnas.2113853119.

315 (10) Haydock, A. K.; Porat, I.; Whitman, W. B.; Leigh, J. A. Continuous culture of *Methanococcus*
316 *maripaludis* under defined nutrient conditions. *FEMS Microbiol. Lett*. **2004**, *238*, 85–91.
317 https://doi.org/10.1016/j.femsle.2004.07.021.

318 (11) Müller, A. L.; Gu, W.; Patsalo, V.; Deutzmann, J. S.; Williamson, J. R. An alternative resource
319 allocation strategy in the chemolithoautotrophic archaeon *Methanococcus maripaludis*. *Proc.*
320 *Natl. Acad. Sci. U. S. A.* **2021**, 1–8. https://doi.org/10.1073/pnas.2025854118.

321 (12) Kessler, P. S.; Daniel, C.; Leigh, J. A. Ammonia switch-off of nitrogen fixation in the
322 methanogenic archaeon *Methanococcus maripaludis*: mechanistic features and requirement
323 for the novel GlnB Homologues, NifI1 and NifI2. *J. Bacteriol.* **2001**, *183* (3), 882–889.
324 https://doi.org/10.1128/JB.183.3.882-889.2001.

325 (13) Kessler, P. S.; Leigh, J. A. Genetics of nitrogen regulation in *Methanococcus maripaludis*.
326 *Genetics* **1999**, *152* (4), 1343–1351. https://doi.org/10.1093/genetics/152.4.1343.

327 (14) Lie, T. J.; Wood, G. E.; Leigh, J. A. Regulation of *nif* expression in *Methanococcus maripaludis*:
328 roles of the euryarchaeal repressor NrpR, 2-oxoglutarate, and two operators. *J. Biol. Chem.*
329 **2005**, *280* (7), 5236–5241. https://doi.org/10.1074/jbc.M411778200.

330 (15) Goyal, N.; Zhou, Z.; Karimi, I. A. Metabolic processes of *Methanococcus maripaludis* and
331 potential applications. *Microb. Cell Fact.* **2016**, *15* (1), 1–19. https://doi.org/10.1186/s12934-
332 016-0500-0.

333 (16) Lohner, S. T.; Deutzmann, S.; Logan, B. E.; Leigh, J.; Spormann, A. M. Hydrogenase-
334 independent uptake and metabolism of electrons by the archaeon *Methanococcus*
335 *maripaludis*. *The ISME Journal* **2014**, 1673–1681. https://doi.org/10.1038/ismej.2014.82.

336 (17) Moore, B. C.; Leigh, J. A. Markerless mutagenesis in *Methanococcus maripaludis*
337 demonstrates roles for alanine dehydrogenase, alanine racemase, and alanine permease. *J.*
338 *Bacteriol.* **2005**, *187* (3), 972–979. https://doi.org/10.1128/JB.187.3.972-979.2005.

339 (18) Ran, F. A.; Hsu, P. D.; Wright, J.; Agarwala, V.; Scott, D. A.; Zhang, F. Genome engineering
340 using the CRISPR-Cas9 System. *Nat. Protoc.* **2013**, *8* (11), 2281–2308.
341 https://doi.org/10.1038/nprot.2013.143.

342 (19) Shalem, O.; Sanjana, E. N.; Hartenian, E.; Shi, X.; Scott, D. A.; Mikkelsen, T. S.; Heckl, D.; Ebert,
343 B. L.; Root, D. E.; Doench, J. G.; Zhang, F. Genome-scale CRISPR-Cas9 knockout screening in
344 human cells. *Science* **2014**, *343*, 84–88.

345 (20) Decaestecker, W.; Buono, R. A.; Pfeiffer, M. L.; Vangheluwe, N.; Jourquin, J.; Karimi, M.; van
346 Isterdael, G.; Beeckman, T.; Nowack, M. K.; Jacobs, T. B. CRISPR-Tsko: A technique for
347 efficient mutagenesis in specific cell types, tissues, or organs in Arabidopsis. *Plant Cell* **2019**,
348 *31* (12), 2868–2887. https://doi.org/10.1105/tpc.19.00454.

349 (21) Miao, J.; Guo, D.; Zhang, J.; Huang, Q.; Qin, G.; Zhang, X.; Wan, J.; Gu, H.; Qu, L. J. Targeted
350 mutagenesis in rice using CRISPR-Cas system. *Cell Res.* **2013**, *23* (10), 1233–1236.
351 https://doi.org/10.1038/cr.2013.123.

352 (22) Jessop-Fabre, M. M.; Jakočiūnas, T.; Stovicek, V.; Dai, Z.; Jensen, M. K.; Keasling, J. D.;
353 Borodina, I. EasyClone-MarkerFree: A vector toolkit for marker-less integration of genes into
354 *Saccharomyces cerevisiae* via CRISPR-Cas9. *Biotechnol. J.* **2016**, *11* (8), 1110–1117.
355 https://doi.org/10.1002/biot.201600147.

356 (23) Cai, P.; Duan, X.; Wu, X.; Gao, L.; Ye, M.; Zhou, Y. J. Recombination machinery engineering
357 facilitates metabolic engineering of the industrial yeast *Pichia Pastoris*. *Nucleic Acids Res.*
358 **2021**, *49* (13), 7791–7805. https://doi.org/10.1093/nar/gkab535.

359 (24) Gophna, U.; Allers, T.; Marchfelder, A. Finally, archaea get their CRISPR-Cas Toolbox. *Trends*
360 *Microbiol.* **2017**, *25* (6), 430–432. https://doi.org/10.1016/j.tim.2017.03.009.

361 (25) Nayak, D. D.; Metcalf, W. W. Cas9-mediated genome editing in the methanogenic archaeon
362 *Methanosarcina Acetivorans*. *Proc. Natl. Acad. Sci. U. S. A.* **2017**, *114* (11), 2976–2981.
363 https://doi.org/10.1073/pnas.1618596114.

364 (26) Zetsche, B.; Gootenberg, J. S.; Abudayyeh, O. O.; Slaymaker, I. M.; Makarova, K. S.;
365 Essletzbichler, P.; Volz, S. E.; Joung, J.; van der Oost, J.; Regev, A.; Koonin, E. V.; Zhang, F. Cpf1
366 is a single RNA-guided endonuclease of a Class 2 CRISPR-Cas system. *Cell* **2015**, *163* (3), 759–
367 771. https://doi.org/10.1016/J.CELL.2015.09.038.

368 (27) Zetsche, B.; Heidenreich, M.; Mohanraju, P.; Fedorova, I.; Kneppers, J.; DeGennaro, E. M.;
369 Winblad, N.; Choudhury, S. R.; Abudayyeh, O. O.; Gootenberg, J. S.; Wu, W. Y.; Scott, D. A.;
370 Severinov, K.; van der Oost, J.; Zhang, F. Multiplex gene editing by CRISPR–Cpf1 using a single
371 crRNA array. *Nat. Biotechnol.* **2016**, *35* (1), 31–34. https://doi.org/10.1038/nbt.3737.

372 (28) Fonseca, D. R.; Halim, M. F. A.; Holten, M. P.; Costa, K. C. Type IV-like pili facilitate
373 transformation in naturally competent archaea. *J. Bacteriol.* **2020**, *202* (21), 1–12.

374 https://doi.org/10.1128/JB.00355-20.

375 (29) Dodsworth, J. A.; Leigh, J. A. Regulation of nitrogenase by 2-oxoglutarate-reversible, direct
376 binding of a PII - like nitrogen sensor protein to dinitrogenase. *Proc. Natl. Acad. Sci. U. S. A.*
377 **2006**, *103* (26), 9779–9784. https://doi.org/10.1073/pnas.0602278103.

378 (30) White, M. F.; Allers, T. DNA repair in the archaea - an emerging picture. *FEMS Microbiol. Rev.*
379 **2018**, *42* (4), 514–526. https://doi.org/10.1093/femsre/fuy020.

380 (31) Tumbula, D. L.; Makula, R. A.; Whitman, W. B. Transformation of *Methanococcus maripaludis*
381 and identification of a *Pst* I-like restriction system. *FEMS Microbiol. Lett.* **1994**, *121* (3), 309–
382 314. https://doi.org/10.1111/j.1574-6968.1994.tb07118.x.

383 (32) Kohler, P. R. A.; Metcalf, W. W. Genetic manipulation of *Methanosarcina spp*. *Front.*
384 *Microbiol.* **2012**, *3* (JUL), 1–9. https://doi.org/10.3389/fmicb.2012.00259.

385 (33) Lie, T. J.; Leigh, J. A. A novel repressor of *nif* and *glnA* expression in the methanogenic
386 archaeon *Methanococcus maripaludis. Mol. Microbiol.* **2003**, *47* (1), 235–246.
387 https://doi.org/10.1046/j.1365-2958.2003.03293.x.

388 (34) Lie, T. J.; Leigh, J. A. Regulatory response of *Methanococcus maripaludis* to alanine, an
389 Intermediate nitrogen source. *J. Bacteriol.* **2002**, *184* (19), 5301–5306.
390 https://doi.org/10.1128/JB.184.19.5301-5306.2002.

391 (35) Lyu, Z.; Chou, C.-W.; Shi, H.; Wang, L.; Ghebreab, R.; Phillips, D.; Yan, Y.; Duin, E. C.; Whitman,
392 W. B. Assembly of methyl-coenzyme M reductase in the methanogenic archaeon
393 *Methanococcus maripaludis*. *J. Bacteriol.* **2018**, *12; 200 (7)* :e00746-17.
394 https://doi.org/10.1128/JB.00746-17.

395 (36) Lienemann, M.; Deutzmann, J. S.; Milton, R. D.; Sahin, M.; Spormann, A. M. Mediator-free
396 enzymatic electrosynthesis of formate by the *Methanococcus maripaludis* heterodisulfide
397 reductase supercomplex. *Bioresour. Technol.* **2018**, *254*, 278–283.
398 https://doi.org/10.1016/j.biortech.2018.01.036.

399 (37) Akinyemi, T. S.; Shao, N.; Lyu, Z.; Drake, I. J.; Liu, Y.; Whitman, W. B. Tuning gene expression
400 by phosphate in the methanogenic archaeon *Methanococcus maripaludis*. *ACS Synth. Biol.*
401 **2021**. *10*(11), 3028–3039. https://doi.org/10.1021/acssynbio.1c00322.

402 (38) Ding, Y.; Berezuk, A.; Khursigara, C. M.; Jarrell, K. F.; Maupin-furlow, J. A. Bypassing the need
403 for the transcriptional activator EarA through a spontaneous deletion in the BRE portion of
404 the *fla* operon promoter in *Methanococcus maripaludis*. *Front. Microbiol*. **2017**, *8* (July), 1–10.
405 https://doi.org/10.3389/fmicb.2017.01329.

406 (39) B.Whitman, W.; Shieh, J.; Sohn, S.; Caras, D. S.; Premachandran, U. Isolation and
407 characterization of 22 mesophilic *Methanococci*. *Syst. Appl. Microbiol.* **1986**, *7* (2–3), 235–
408 240.

409 (40) Gibson, D. G.; Young, L.; Chuang, R. Y.; Venter, J. C.; Hutchison, C. A.; Smith, H. O. Enzymatic
410 assembly of DNA molecules up to several hundred kilobases. *Nat. Methods.* **2009**, *6* (5), 343–
411 345. https://doi.org/10.1038/nmeth.1318.

412 (41) Labun, K.; Montague, T. G.; Krause, M.; Cleuren, Y. N. T.; Valen, E. CHOPCHOP v3 : Expanding
413 the CRISPR web toolbox beyond genome editing. *Nucleic Acids Res.* **2019**, *47*, 171–174.
414 https://doi.org/10.1093/nar/gkz365.

415 (42) Long, F.; Wang, L.; Lupa, B.; Whitman, W. B. A flexible system for cultivation of
416 *Methanococcus* and other formate-utilizing methanogens. *Archaea* **2017**, *2017*, 1–12.

https://doi.org/10.1155/2017/7046026.

419 **Figure legends**

420

421 **Figure 1.** Features and transformation efficiency of the CRISPR/LbCas12a plasmid pMM002P. a) The
422 schematic diagram of pMM002P. The uracil phosphoribosyltransferase (*upt*) from *M. maripaludis* S2
423 as a counter-selective marker is co-expressed with the codon-optimized puromycin *N*-
424 acetyltransferase (*pac*) under the $P_{mcr}$ promoter[4]. LbCas12a expression is driven by the promoter $P_{hdr}$
425 from *Methanococcus voltae* A3. The histone promoter $P_{hmv}$ from *M. voltae* A3 is used to express the
426 gRNA. For inserting the required gRNA, two *PaqC* I sites are placed between the direct repeat
427 sequence and the synthetic terminator in the opposite direction for spacer fusion (not displayed).
428 The gRNA of the plasmid pMM002P containing two *PaqC* I sites is designed to not target the native
429 chromosome. An *Mre* I restriction site was assigned between the promoters $P_{hdr}$ and $P_{hmv}$ for RF
430 insertion, if needed. b) Cleavage test with transformed plasmid pMM002P, using 0, 1, or 2 gRNA
431 carried out in triplicates. The error bars represent the standard deviation (n=3).

432

433 **Figure 2.** Transformation efficiency and positive rate in relation to the length and position of the RF.
434 a) Variation of the length of the homologous arms flanking the RF, whereby the distance from the RF
435 to DSB is 25 bp. b) Variation of the distance between the RF to the DSB, whereby the length of the
436 homologous arms is 1000 bp. For the 25 bp distance experiment, same plasmid has been used as for
437 the 1000 bp length experiment in a.

438 The error bars for the transformation efficiency represent the standard deviation (n=3). The
439 numbers above the the bars indicate the positive rate (fraction of correctly edited colonies per
440 colonies tested via PCR).

441

442 **Figure 3.** Replacing the whole ORF of the flagellum operon by *uidA* from *E. coli*. p002-218 expresses
443 one gRNA, p002-226 expresses two gRNAs. "uidA" indicates that the RF is present on the
444 corresponding plasmid. The error bars for the transformation efficiency represent the standard
445 deviation (n=3). The numbers above the bars indicate the positive rate (fraction of correctly edited
446 colonies per colonies tested via PCR).

447

448 **Figure 4.** Quantification of promoter strengths for the two different growth conditions formate or
449 $H_2$+$CO_2$, measured after the culture has reached $OD_{600}$ = ca. 0.5. The promoters mcr_JJ, mcrR_JJ and
450 fla_JJ are from *M. maripaludis* JJ. The remaining promoters are from *Methanococcus vannielii* SB.
451 Error bars represent the standard deviation (n=3).

452

453

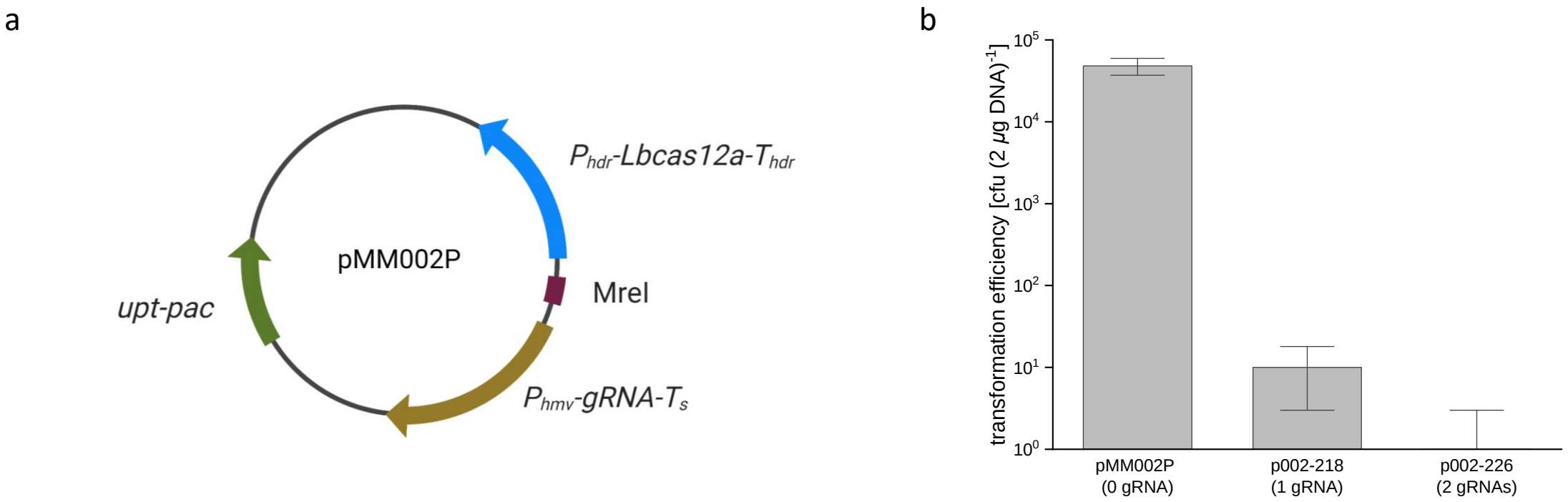


**Figure 1.** Features and transformation efficiency of the CRISPR/LbCas12a plasmid pMM002P. a) The schematic diagram of pMM002P. The uracil phosphoribosyltransferase (*upt*) from *M. maripaludis* S2 as a counter-selective marker is co-expressed with the codon-optimized puromycin *N*-acetyltransferase (*pac*) under the $P_{mcr}$ promoter[4]. LbCas12a expression is driven by the promoter $P_{hdr}$ from *Methanococcus voltae* A3. The histone promoter $P_{hmv}$ from *M. voltae* A3 is used to express the gRNA. For inserting the required gRNA, two *PaqC* I sites are placed between the direct repeat sequence and the synthetic terminator in the opposite direction for spacer fusion (not displayed). The gRNA of the plasmid pMM002P containing two *PaqC* I sites is designed to not target the native chromosome. An *Mre* I restriction site was assigned between the promoters $P_{hdr}$ and $P_{hmv}$ for RF insertion, if needed. b) Cleavage test with transformed plasmid pMM002P, using 0, 1, or 2 gRNA carried out in triplicates. The error bars represent the standard deviation (n=3).

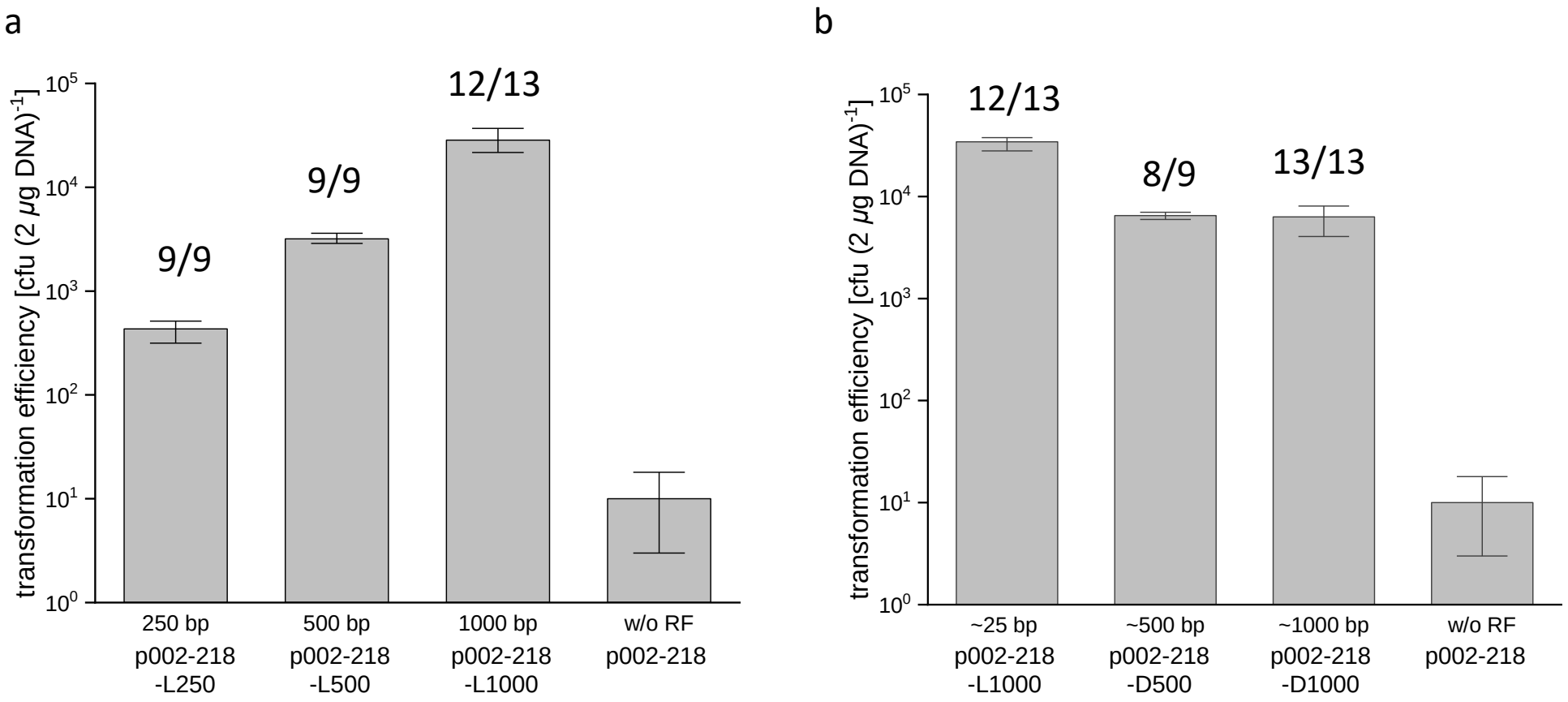


**Figure 2.** Transformation efficiency and positive rate in relation to the length and position of the RF. a) Variation of the length of the homologous arms flanking the RF, whereby the distance from the RF to DSB is 25 bp. b) Variation of the distance between the RF to the DSB, whereby the length of the homologous arms is 1000 bp. For the 25 bp distance experiment, same plasmid has been used as for the 1000 bp length experiment in a.
The error bars for the transformation efficiency represent the standard deviation (n=3). The numbers above the the bars indicate the positive rate (fraction of correctly edited colonies per colonies tested via PCR).

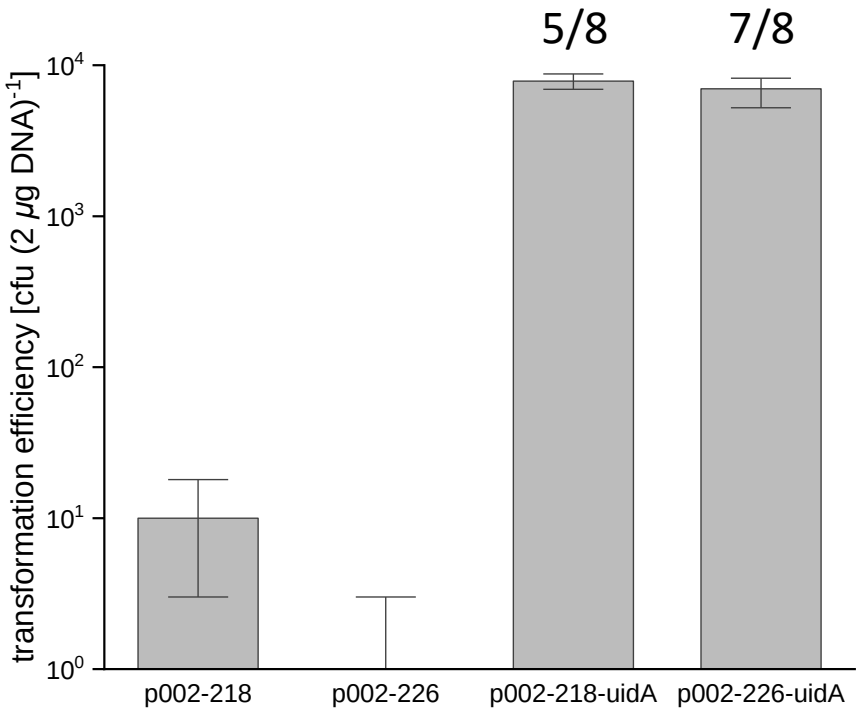


**Figure 3.** Replacing the whole ORF of the flagellum operon by *uidA* from *E. coli*. p002-218 expresses one gRNA, p002-226 expresses two gRNAs. “uidA” indicates that the RF is present on the corresponding plasmid. The error bars for the transformation efficiency represent the standard deviation (n=3). The numbers above the bars indicate the positive rate (fraction of correctly edited colonies per colonies tested via PCR).

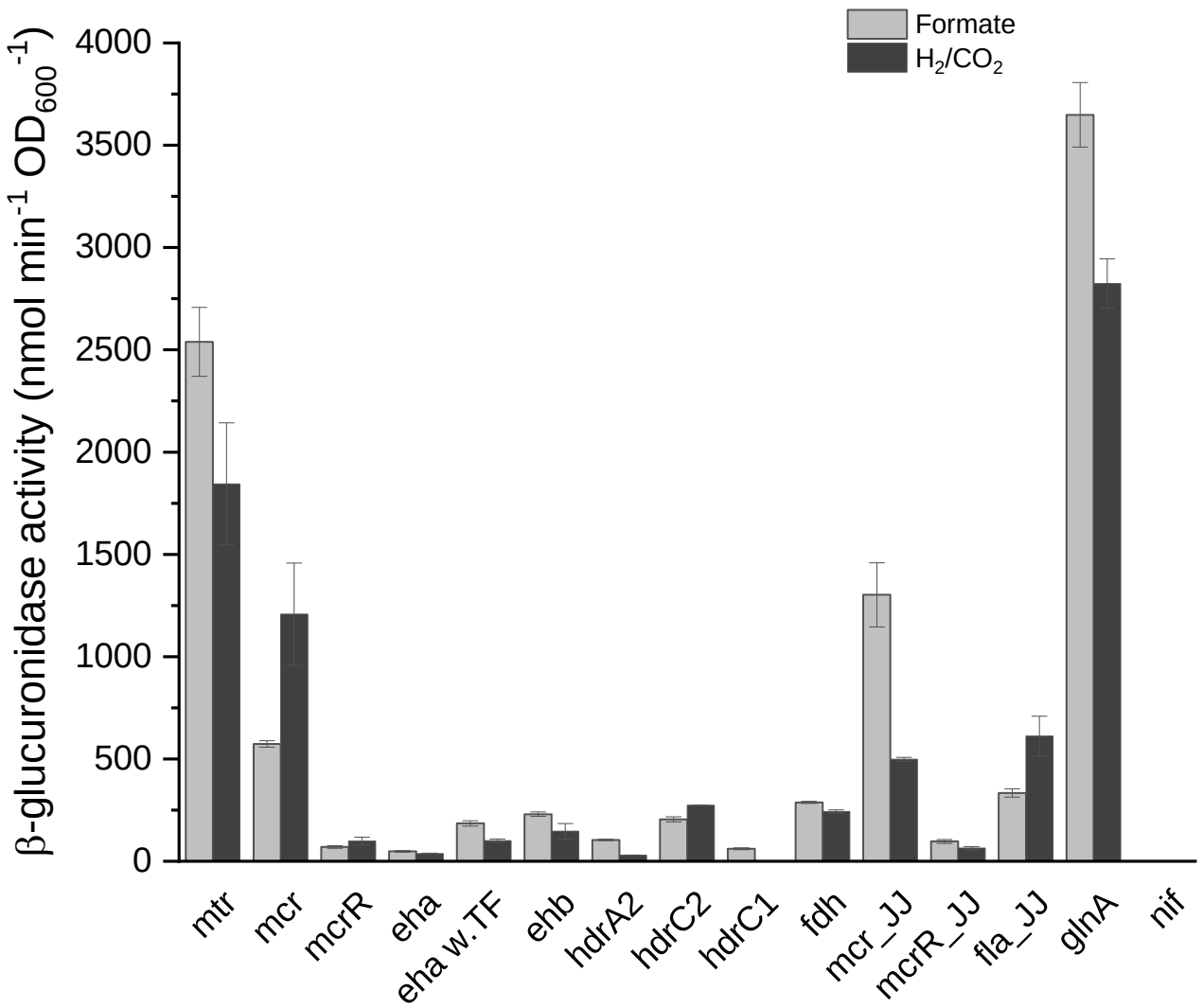


**Figure 4.** Quantification of promoter strengths for the two different growth conditions formate or $H_2$+$CO_2$, measured after the culture has reached $OD_{600}$ = ca. 0.5. The promoters mcr_JJ, mcrR_JJ and fla_JJ are from *M. maripaludis* JJ. The remaining promoters are from *Methanococcus vannielii* SB. Error bars represent the standard deviation (n=3).

**Table S1.** Plasmid list

| Plasmid | Description | Reference |
|---|---|---|
| pLW40 | *E. coli*/*M. maripaludis* shuttle vector; the backbone of pMM002P | [1] |
| pMEV4 | *E. coli*/*M. maripaludis* shuttle vector, only replicates in *M. maripaludis* S0001[2], carrying codon-optimized *pac* | [3] |
| pMEV4mTs | Derived from pMEV4 carrying the synthetic terminator (*Ts*) | Provided by Prof. Whitman |
| pY016 | Nucleic acid sequence source of LbCas12a | [4] |
| pX165 | Nucleic acid sequence source of SpCas9 | [5] |
| pMM002P | CRISPR/LbCas12a toolbox plasmid | This study |
| pMM005 | CRISPR/SpCas9 toolbox plasmid | This study |
| p002-218 | pMM002P containing a guide sequence 5'-CCCACAGATGAATATACTCATTCC targeting to *flaI* | This study |
| p002-226 | pMM002P containing guide sequences 5'-GATATACCCGACACAATGATATCG and 5' -CTGTTCCCACTCTACTAATTAAAA targeting to *flaJ* and *flaD* | This study |
| p002-218-L1000 | p002-218, 1000 bp long homologous arms on each side, 25 bp from the RF to DSB | This study |
| p002-218-L500 | p002-218, 500 bp long homologous arms on each side, 25 bp from the RF to DSB | This study |
| p002-218-L250 | p002-218, 250 bp long homologous arms on each side, 25 bp from the RF to DSB | This study |
| p002-218-D500 | p002-218, 1000 bp long homologous arms on each side, 500 bp from the RF to DSB | This study |
| p002-218-D1000 | p002-218, 1000 bp long homologous arms on each side, 1000 bp from the RF to DSB | This study |
| p002-218-uidA | p002-218, $P_{fla_JJ}$-*uidA*-$T_{fla}$; the 1000 bp homologous arms on each side covers the promoter and the terminator of the flagellum operon | This study |
| p002-226-uidA | p002-226, $P_{fla_JJ}$-*uidA*-$T_{fla}$; the 1000 bp homologous arms on each side covers the promoter and the terminator of the flagellum operon | This study |
| p002-253 | pMM002P containing a guide sequence 5'-AATGCAAGCTACAACTGTGTAGAC targeting to *acs* | This study |
| p002-247 | pMM002P containing a guide sequence 5'-AGTGATACCTAACAGCCCTTTCTC targeting to *nrpR* | This study |
| pPmtr-uidA | suicide plasmid containing "$P_{mtr}$-*uidA*" cassette, 1000 bp long homologous arms on each side, the promoter is from *M. vannielli* SB | This study |
| pPmcr-uidA | suicide plasmid containing "$P_{mcr}$-*uidA*" cassette, 1000 bp long homologous arms on each side, the promoter is from *M. vannielli* SB | This study |
| pPmcrR-uidA | suicide plasmid containing "$P_{mcrR}$-*uidA*" cassette, 1000 bp long homologous arms on each side, the promoter is from *M. vannielli* SB | This study |

| | | |
|---|---|---|
| pPhdrC1-uidA | suicide plasmid containing "$P_{hdrC1}$-*uidA*" cassette, 1000 bp long homologous arms on each side, the promoter is from *M. vannielli* SB | This study |
| pPhdrC2-uidA | suicide plasmid containing "$P_{hdrC2}$-*uidA*" cassette, 1000 bp long homologous arms on each side, the promoter is from *M. vannielli* SB | This study |
| pPhdrA2-uidA | suicide plasmid containing "$P_{hdrA2}$-*uidA*" cassette, 1000 bp long homologous arms on each side, the promoter is from *M. vannielli* SB | This study |
| pPfdh-uidA | suicide plasmid containing "$P_{fdh}$-*uidA*" cassette, 1000 bp long homologous arms on each side, the promoter is from *M. vannielli* SB | This study |
| pPeha-uidA | suicide plasmid containing "$P_{eha}$-*uidA*" cassette, 1000 bp long homologous arms on each side, the promoter is from *M. vannielli* SB | This study |
| pPeha w.TF-uidA | suicide plasmid containing "$P_{eha\ w.TF}$-*uidA*" cassette, 1000 bp long homologous arms on each side, the promoter is from *M. vannielli* SB | This study |
| pPehb-uidA | suicide plasmid containing "$P_{ehb}$-*uidA*" cassette, 1000 bp long homologous arms on each side, the promoter is from *M. vannielli* SB | This study |
| pPglnA-uidA | suicide plasmid containing "$P_{glnA}$-*uidA*" cassette, 1000 bp long homologous arms on each side, the promoter is from *M. vannielli* SB | This study |
| pPnif-uidA | suicide plasmid containing "$P_{nif}$-*uidA*" cassette, 1000 bp long homologous arms on each side, the promoter is from *M. vannielli* SB | This study |
| pPmcr_JJ-uidA | suicide plasmid containing "$P_{mcr_JJ}$-*uidA*" cassette, 1000 bp long homologous arms on each side, the promoter is from *M. maripaludis JJ* | This study |
| pPmcrR_JJ-uidA | suicide plasmid containing "$P_{mcrR_JJ}$-*uidA*" cassette, 1000 bp long homologous arms on each side, the promoter is from *M. maripaludis JJ* | This study |
| pPfla_JJ-uidA | suicide plasmid containing "$P_{fla_JJ}$-*uidA*" cassette, 1000 bp long homologous arms on each side, the promoter is from *M. maripaludis JJ* | This study |
| pΔnrpR | suicide plasmid containing deletion cassette of *nrpR*, a $P_{mcr}$ promoter was placed between the homologous arms to drive the expression of *rlmE*, which is at the downstream of *nrpR* | This study |
| p005-380 | pMM005 containing guide sequences 5'-tattgagatgtgtttccggg targeting to *alr* | This study |
| p4.2k | suicide plasmid containing a 4.2 kb insertion flanking with ca. 1000 bp upstream of *ald* and 1000 bp downstream of *alr* | This study |

**Table S2.** Strain list

| Strain | Genotype | Remarks | Reference |
|---|---|---|---|
| S2 | wildtype | Used as PCR template for *upt* gene | [6] |
| SB | *Methanococcus vannielii* | Used as PCR template for promoters | Purchased from DSMZ |
| A3 | *Methanococcus voltae* | Used as PCR template for promoter and terminator for Cas protein expression | Provided by Prof. Whitman |
| JJΔupt | Δ*upt* | | [7] |
| JL1000 | Δ*upt* Δ*flaI(849-904)::gcggccgc* with p002-218-L1000 | JJΔupt was transformed with p002-218-L1000 | This study |
| JL500 | Δ*upt* Δ*flaI(849-904)::gcggccgc* with p002-218-L500 | JJΔupt was transformed with p002-218-L500 | This study |
| JL250 | Δ*upt* Δ*flaI(849-904)::gcggccgc* with p002-218-L250 | JJΔupt was transformed with p002-218-L250 | This study |
| JD500 | Δ*upt* Δ*flaI(378-1379)::gcggccgc* with p002-218-D500 | JJΔupt was transformed with p002-218-D500 | This study |
| JD1000 | Δ*upt* Δ*flaH(621-693)IJ(1-179)::gcggccgc* with p002-218-D1000 | JJΔupt was transformed with p002-218-D1000 | This study |
| J218U | Δ*upt* Δ*flaB1B2B3CDEFGHIJ::uidA* | JJΔupt was transformed with p002-218-uidA, plasmid was removed afterwards. | This study |
| J226U | Δ*upt* Δ*flaB1B2B3CDEFGHIJ::uidA* | JJΔupt was transformed with p002-226-uidA, plasmid was removed afterwards. | This study |
| Jmtr | Δ*upt* Δ*acs(107-1075)::*$P_{mtr}$*-uidA* | JJΔupt was transformed with p002-253 and pPmtr-uidA, plasmid was removed afterwards. | This study |
| Jmcr | Δ*upt* Δ*acs(107-1075)::*$P_{mcr}$*-uidA* | JJΔupt was transformed with p002-253 and pPmcr-uidA, plasmid was removed afterwards. | This study |
| JmcrR | Δ*upt* Δ*acs(107-1075)::*$P_{mcrR}$*-uidA* | JJΔupt was transformed with p002-253 and pPmcrR-uidA, plasmid was removed afterwards. | This study |
| JhdrC1 | Δ*upt* Δ*acs(107-1075)::*$P_{hdrC1}$*-uidA* | JJΔupt was transformed with p002-253 and pPhdrC1-uidA, plasmid was removed afterwards. | This study |
| JhdrC2 | Δ*upt* Δ*acs(107-1075)::*$P_{hdrC2}$*-uidA* | JJΔupt was transformed with p002-253 and pPhdrC2-uidA, plasmid was removed afterwards. | This study |

| | | | |
|---|---|---|---|
| JhdrA2 | Δ*upt* Δ*acs(107-1075)::*$P_{hdrA2}$*-uidA* | JJΔupt was transformed with p002-253 and pPhdrA2-uidA, plasmid was removed afterwards. | This study |
| Jfdh | Δ*upt* Δ*acs(107-1075)::*$P_{fdh}$*-uidA* | JJΔupt was transformed with p002-253 and pPfdh-uidA, plasmid was removed afterwards. | This study |
| Jeha | Δ*upt* Δ*acs(107-1075)::*$P_{eha}$*-uidA* | JJΔupt was transformed with p002-253 and pPeha-uidA, plasmid was removed afterwards. | This study |
| Jehawtf | Δ*upt* Δ*acs(107-1075)::*$P_{eha\ w.TF}$*-uidA* | JJΔupt was transformed with p002-253 and pPeha w.TF-uidA, plasmid was removed afterwards. | This study |
| Jehb | Δ*upt* Δ*acs(107-1075)::*$P_{ehb}$*-uidA* | JJΔupt was transformed with p002-253 and pPehb-uidA, plasmid was removed afterwards. | This study |
| JglnA | Δ*upt* Δ*acs(107-1075)::*$P_{glnA}$*-uidA* | JJΔupt was transformed with p002-253 and pPglnA-uidA, plasmid was removed afterwards. | This study |
| Jnif | Δ*upt* Δ*acs(107-1075)::*$P_{nif}$*-uidA* | JJΔupt was transformed with p002-253 and pPnif-uidA, plasmid was removed afterwards. | This study |
| JmcrJ | Δ*upt* Δ*acs(107-1075)::*$P_{mcr_JJ}$*-uidA* | JJΔupt was transformed with p002-253 and pPmcr_JJ-uidA, plasmid was removed afterwards. | This study |
| JmcrRJ | Δ*upt* Δ*acs(107-1075)::*$P_{mcrR_JJ}$*-uidA* | JJΔupt was transformed with p002-253 and pPmcrR_JJ-uidA, plasmid was removed afterwards. | This study |
| JflaJ | Δ*upt* Δ*acs(107-1075)::*$P_{fla_JJ}$*-uidA* | JJΔupt was transformed with p002-253 and pPfla_JJ-uidA, plasmid was removed afterwards. | This study |
| JnifΔnrpR | Δ*upt* Δ*nrpR* Δ*acs(107-1075)::*$P_{nif}$*-uidA* | Jnif was transformed with p002-247 and pΔnrpR | This study |

**Table S3.** plasmid maps

| Plasmid | link |
|---|---|
| pMM002P | https://benchling.com/s/seq-NcNgENuHGpjcjuVSBU0e?m=slm-uWqdWXhT0CNxlHaCyTYG |
| pMM005 | https://benchling.com/s/seq-hvquLQ7RbCe0LrHLvgUG?m=slm-Uljuux0W4UWZCD8H0UbE |
| pPmtr-uidA | https://benchling.com/s/seq-0Gomnk1heQqOZcCU6GRn?m=slm-dHj8kpnVmpgyZ1LyXbNf |
| pPmcr-uidA | https://benchling.com/s/seq-W11SbMBtaTdab5nlcUC9?m=slm-gmg7fHunIevaxHSKpRLf |
| pPmcrR-uidA | https://benchling.com/s/seq-zpHKgTXargZcOH0sg26M?m=slm-b8KraXsjOZP1H77qMZ2N |
| pPhdrC1-uidA | https://benchling.com/s/seq-7vfw1HM5KaJn0JQZxqKr?m=slm-ACTIrP1pfkZRr5MR2y0T |
| pPhdrC2-uidA | https://benchling.com/s/seq-GECSSScdMhnf9XM0i7dH?m=slm-bF0EK8QlLhtSH4lvUW21 |
| pPhdrA2-uidA | https://benchling.com/s/seq-Jwx0H7YJcMCzA42eJPF6?m=slm-cwKCm0LKbQLv1cN4IIaC |
| pPfdh-uidA | https://benchling.com/s/seq-DOMwbRZ6WALbE3SHTTMF?m=slm-sUQWlj4qbdmmL74pSb1Q |
| pPeha-uidA | https://benchling.com/s/seq-vPCMYrXjr9PiLKxHatOs?m=slm-UbqyKGuyakFfSQ4STlse |
| pPeha w.TF-uidA | https://benchling.com/s/seq-TtXDra2oDlyADm8eS7ns?m=slm-CEUoenlUGVfMb8BPeabC |
| pPehb-uidA | https://benchling.com/s/seq-tDXok4O6Ric798CaMapy?m=slm-Hd9WyxMjMk7omegb0obG |
| pPglnA-uidA | https://benchling.com/s/seq-RcddggPTElJMqlZ2s6Eh?m=slm-JKc8i5HNtjdRbuw51yn1 |
| pPnif-uidA | https://benchling.com/s/seq-iaa8yge2Lqaj3XpOCt0Y?m=slm-e7qq4iYbyZtirETKuQt0 |
| pPmcr_JJ-uidA | https://benchling.com/s/seq-6sP4BHn8cSssampgokXB?m=slm-GELjQGAhiabG2JUlaKCl |
| pPmcrR_JJ-uidA | https://benchling.com/s/seq-3wN9rk0VvzFd5cZO1UxY?m=slm-aHvtqEanTqm85apTBcJm |
| pPfla_JJ-uidA | https://benchling.com/s/seq-D6xKkW9YqDEBIvTbz046?m=slm-68Z2g0Tdg8d9wlolLIAX |
| pΔnrpR | https://benchling.com/s/seq-ZaGqJIBsQxrGJb9RARmb?m=slm-APrpwwhfkbpBKSUMw7Qs |

**Table S4.** Primers used for pMM002P construction

| Fragment | Subfragment | Primer | Sequence (5'->3') | Template |
|---|---|---|---|---|
| F1 | | P1 | CTTCTTCAGGGAGCTCGAGATAAGAATTACTAGATCGGAAAATTCAGTAATGCAAAAACAC | *Methanococcus voltae* A3 |
| | | P2 | TTTAATTAAGTATTTTAATTATTCTTTTTTCATTATTTTATTAAGTTATTAC | |
| F2 | F2.1 | P3 | GTAATAACTTAATAAAATAATGAAAAAAGAATAATTAAAATACTTAATTAAATTAGCTGGTCTGGGCGTACTC | pY016 |
| | | P4 | GCCCTGATGAGCCTGATGCTTCAGATGCGGAACAGCATCAC | |
| | F2.2 | P5 | GTGATGCTGTTCCGCATCTGAAGCATCAGGCTCATCAGGGC | pY016 |
| | | P6 | GTGAAGGTGGAGAAGCAGGTTTATCAGAAGTTCGAGAAGATGCTG | |
| | F2.3 | P7 | CAGCATCTTCTCGAACTTCTGATAAACCTGCTTCTCCACCTTCAC | pY016 |
| | | P8 | GGATAAGAAGTACGCCAAGTGCTTACAGAAGATCGACAAGGACGATG | |
| | F2.4 | P9 | CATCGTCCTTGTCGATCTTCTGTAAGCACTTGGCGTACTTCTTATCC | pY016 |
| | | P10 | CCTTCAAGAAGATCGGCTCCTTTTCTTTAGAGCAGTTACAGGAGTACGCCGACGCCG | |
| | F2.5 | P11 | CGGCGTCGGCGTACTCCTGTAACTGCTCTAAAGAAAAGGAGCCGATCTTCTTGAAGG | pY016 |
| | | P12 | GTTTAAGCCACTGTATAAGCAGGTTCTGAGCGATCGGGAGTCTCTG | |
| | F2.6 | P13 | CAGAGACTCCCGATCGCTCAGAACCTGCTTATACAGTGGCTTAAAC | pY016 |
| | | P14 | ATATATATACCTATATAGTGTCGAGGTGTAATAATATGAGCAAGCTGGAGAAGTTTAC | |
| F3 | F3.1 | P15 | ATTATTACACCTCGACACTATATAGGTATATATAT | *Methanococcus voltae* A3 |
| | | P16 | GTTATATTTTGATCGATCAGCTGAATTAACGCCGGCGAATTTTATTAAATTATCATATAACTATATAAATTTATC | |
| | F3.2 | P17 | AATTCGCCGGCGTTAATTCAGCTGATCGATCAAAATATAAC | pMEV4 |
| | | P18 | CAATGCAGGTGCGGATCCTCACCTGCGCATATCTACACTTAGTAGAAATTCACTCTAGTATTAG | |
| | F3.3 | P19 | ATGCGCAGGTGAGGATCCGCACCTGCATTGGATATAGCAAAAGTGGGACTTAAGTTCC | pMEV4mTs |
| | | P20 | GGAAGGTCGTCTCCTCTAGT | |
| | F3.4 | P21 | AAACTAGAGGAGACGACCTTCCATGATAAAAGATGAAAGATGGGAAGGAG | *Methanococcus maripaludis* S2 |
| | | P22 | GTTGGTTTATATTCTGTCATGCATTTCACCTATTTTATTCTAAATTGTGCATTTGTGGGAGC | |
| | F3.5 | P23 | AATAGGTGAAATGCATGACAGAATATAAACCAACAGTTAGATTAGC | pMEV4 |
| | | P24 | CGGCTTCGGTCGGAGCCATGGTTATGCTCCTGGTTTTCTTGTCATAC | |

The fragment F1, subfragments F2.1 to F2.6, and F3.1 to F3.5 were amplified by normal PCR. The fragments F2 and F3 were constructed by jointing F2.1 to F2.6 and F3.1 to F3.5 together by overlap PCR. pMM002P was constructed by assembling NcoI/BcuI digested pLW40, F1, F2, F3 by Gibson cloning[8].

**Table S5.** Primers used for pMM005 construction

| Fragment | Subfragment | Primer | Sequence (5'->3') | Template |
|---|---|---|---|---|
| F1 | | P1 | CTTCTTCAGGGAGCTCGAGATAAGAATTACTAGATCGGAAAATTCAGTAATGCAAAAACAC | *Methanococcus voltae* A3 |
| | | P2 | TTTAATTAAGTATTTTAATTATTCTTTTTTCATTATTTTATTAAGTTATTAC | |
| F4 | F4.1 | P25 | GTAATAACTTAATAAAATAATGAAAAAAGAATAATTAAAATACTTAATTAAATTAGTCGCCTCCCAGCTGAG | pX165 |
| | | P26 | GAGAATGCTGGCCTCTGCCGGCGAACTTCAGAAGGGAAACGAACTGG | |
| | F4.2 | P27 | AGGGCCAGTTCGTTTCCCTTCTGAAGTTCGCCGGCAGAGGCC | pX165 |
| | | P28 | GAAAACACCCAGCTTCAGAACGAGAAGCTGTACCTGTACTACCTTCAGAATGGGCGGGATATGTAC | |
| | F4.3 | P29 | CTGAAGGTAGTACAGGTACAGCTTCTCGTTCTGAAGCTGGGTGTTTTCCACGG | pX165 |
| | | P30 | AGCCCCGCCATTAAGAAGGGCATCCTTCAGACAGTGAAGGTGGTGG | |
| | F4.4 | P31 | CTCGTCCACCACCTTCACTGTCTGAAGGATGCCCTTCTTAATGGC | pX165 |
| | | P32 | ACCTGGCCGAGGATGCCAAACTTCAGCTGAGCAAGGACACCTAC | |
| | F4.5 | P33 | GTCGTCGTAGGTGTCCTTGCTCAGCTGAAGTTTGGCATCCTCGGCCAG | pX165 |
| | | P34 | CATCAATCCATATATTATATATATACCTATATAGTGTCGAGGTGTAATAATATGGACAAGAAGTACAGCATCG | |
| F5 | F3.1 | P15 | ATTATTACACCTCGACACTATATAGGTATATATAT | *Methanococcus voltae* A3 |
| | | P16 | GTTATATTTTGATCGATCAGCTGAATTAACGCCGGCGAATTTTATTAAATTATCATATAACTATATAAATTTATC | |
| | F5.1 | P17 | AATTCGCCGGCGTTAATTCAGCTGATCGATCAAAATATAAC | pMEV4 |
| | | P35 | TGATAACGGACTAGCCTTATTTTAACTTGCTATTTCTAGCTCTAAAACCAATGCAGGTGCGGATCCTCACCTGCGCATCACTCTAGTATTAGTTATCTATAAAATTATAATATCAATAGC | |
| | F5.2 | P36 | AGCAAGTTAAAATAAGGCTAGTCCGTTATCAACTTGAAAAAGTGGCACCGAGTCGGTGCTTTTGATATAGCAAAAGTGGGACTTAAGTTCCC | pMEV4mTs |
| | | P20 | GGAAGGTCGTCTCCTCTAGT | |
| | F3.4 | P21 | AAACTAGAGGAGACGACCTTCCATGATAAAAGATGAAAGATGGGAAGGAG | *Methancoccus maripaludis* S2 |
| | | P22 | GTTGGTTTATATTCTGTCATGCATTTCACCTATTTTATTCTAAATTGTGCATTTGTGGGAGC | |
| | F3.5 | P23 | AATAGGTGAAATGCATGACAGAATATAAACCAACAGTTAGATTAGC | pMEV4 |
| | | P24 | CGGCTTCGGTCGGAGCCATGGTTATGCTCCTGGTTTTCTTGTCATAC | |

The subfragments F4.1 to F4.5, and F5.1 to F5.2 were amplified by normal PCR. The fragments F4 and F5 were constructed by jointing F4.1 to F4.5 and F3.1, F5.1, F5.2, F3.4 and F3.5 together by overlap PCR. pMM005 was constructed by assembling NcoI/BcuI digested pLW40, F1, F4, F5 by Gibson cloning[8].

**Table S6**. The rest of primers used in this study

| Primer | Sequence (5'->3') | |
|---|---|---|
| CR227 | GCTTATAATGTTTTTAATTTTTAAAAACAGATAAATTTATATAGTTATATGATAATTTAATAAAATTCGCCCAAATTTTGTAATGAATATGTGGAGTCTTTCATTT | L1000 |
| CR228 | GTACAATGTCTGCTCAGACTGCGCGGCCGCCTGCGTCAGGAAAAACTACTTC | |
| CR229 | GAAGTAGTTTTTCCTGACGCAGGCGGCCGCGCAGTCTGAGCAGACATTGTAC | |
| CR230 | GTTATTTATGTTATATTTTGATCGATCAGCTGAATTAACGCCGGCAACTTATTCTTTCGGGGGAAATC | |
| CR231 | GCTTATAATGTTTTTAATTTTTAAAAACAGATAAATTTATATAGTTATATGATAATTTAATAAAATTCGCCGACCGCTGTCTATTGAATAAGC | D250 |
| CR232 | GAATGGGAAGATGAAGGGGACGCGGCCGCGGTCTGTCGAAGGAGCTGTTG | |
| CR233 | CAACAGCTCCTTCGACAGACCGCGGCCGCGTCCCCTTCATCTTCCCATTC | |
| CR234 | GTTATTTATGTTATATTTTGATCGATCAGCTGAATTAACGCCGGGCATACAAGAGCATTTTATGAAAAAGATATTG | |
| CR235 | GCTTATAATGTTTTTAATTTTTAAAAACAGATAAATTTATATAGTTATATGATAATTTAATAAAATTCGCCTTTATCGCATAGACCAAAAGTACTTC | D500 |
| CR236 | CATGGTTGCAAAAGTATCAAGTCAGCGGCCGCCATTACAAGAGGTGTTTTTGAATGG | |
| CR237 | CCATTCAAAAACACCTCTTGTAATGGCGGCCGCTGACTTGATACTTTTGCAACCATG | |
| CR238 | GTTATTTATGTTATATTTTGATCGATCAGCTGAATTAACGCCGGTCTTAATTGAAGGAGAAGAGTCATCC | |
| CR239 | GCTTATAATGTTTTTAATTTTTAAAAACAGATAAATTTATATAGTTATATGATAATTTAATAAAATTCGCCCCATTCAAAAACACCTCTTGTAATGAC | L500 (amplified with CR228 and CR229) |
| CR240 | GTTATTTATGTTATATTTTGATCGATCAGCTGAATTAACGCCGGTTTGACATGGTTGCAAAAGTATCAAG | |
| CR241 | GCTTATAATGTTTTTAATTTTTAAAAACAGATAAATTTATATAGTTATATGATAATTTAATAAAATTCGCCAAAGCAACAGCTCCTTCGAC | L250 (amplified with CR228 and CR229) |
| CR242 | GTTATTTATGTTATATTTTGATCGATCAGCTGAATTAACGCCGGCAAACATTGAATGGGAAGATGAAG | |
| CR243 | GCTTATAATGTTTTTAATTTTTAAAAACAGATAAATTTATATAGTTATATGATAATTTAATAAAATTCGCCATTTTAGACGTATTTTCGTCGAGTTC | $P_{fla_JJ}$-*uidA*-$T_{fla}$ |
| CR244 | GGGGTTTCTACAGGACGTAACATGATTGAACCTCCTAAGTTCACCAG | |
| CR245 | CAGCAGGGAGGCAAACAATGATTTATTTAAAAAATCATTTGAATAGTGAACCG | |
| CR246 | GTTATTTATGTTATATTTTGATCGATCAGCTGAATTAACGCCGGGCAGTTCCAAATTTCAACATTTTATCAC | |
| E275 | ATGTTACGTCCTGTAGAAACCCC | |
| CR31 | TCATTGTTTGCCTCCCTGCTG | |
| CR394 | GGAGAGCAGGCAAAATGTTTAGCTTTTTACCACCTGAAAGAAAAACTTATAC | $P_{nif}$ |
| CR395 | GGGGTTTCTACAGGACGTAACATACTAAAGCCTCTATTGCATCATC | |
| CR396 | GGAGAGCAGGCAAAATGTTTAGTCCTATGAATATTTAAGGAGGCCTTTTGG | $P_{mtr}$ |
| CR398 | GGGGTTTCTACAGGACGTAACATTATTTCACCTCACAATATACGGGAATG | |
| CR399 | GGAGAGCAGGCAAAATGTTTAGATTACCATCTTATTTACTTTTATAAAAATAGTAGTAAGTAG | $P_{mcr}$ |

| | | |
|---|---|---|
| CR400 | GGGGTTTCTACAGGACGTAACATAGGAACCACTCCTATTTTTTTGATATATACATC | |
| CR401 | GGAGAGCAGGCAAAATGTTTAGAGGAACCACTCCTATTTTTTTGATATATAC | $P_{mcrR}$ |
| CR402 | GGGGTTTCTACAGGACGTAACATATTACCATCTTATTTACTTTTATAAAAATAGTAGTAAGTAG | |
| CR403 | GGAGAGCAGGCAAAATGTTTAGAAGAGCATAGTTTATATCGTTTATACCATC | $P_{hdrC1}$ |
| CR404 | GGGGTTTCTACAGGACGTAACATCAGTAACACCTCGAGGATACTTTTG | |
| CR405 | GGAGAGCAGGCAAAATGTTTAGGCACCCGATTTCAACAACC | $P_{hdrC2}$ |
| CR406 | GGGGTTTCTACAGGACGTAACATTCGCTTCACCTCCCTTATAGTTTAATTTTTC | |
| CR407 | GGAGAGCAGGCAAAATGTTTAGGAAATCCCTCGCACATAGAGAAC | $P_{hdrA2}$ |
| CR408 | GGGGTTTCTACAGGACGTAACATGGATTCACCTCCACATATAACAAGTAAG | |
| CR411 | GGAGAGCAGGCAAAATGTTTAGCTGTGAAGAAAGAAACGTTATAGATGG | $P_{fdh}$ |
| CR412 | GGGGTTTCTACAGGACGTAACATTAATCATCACCGTTAAATTATGTGTGAC | |
| CR413 | GGAGAGCAGGCAAAATGTTTAGAAAAAATCACCTTAATCAAATTTTGAAAATGC | $P_{eha}$ |
| CR414 | GGGGTTTCTACAGGACGTAACATTTTACCACGATTTAGTCTACAAGACTTTAAATTATTTC | |
| CR414L | GGGGTTTCTACAGGACGTAACATTAATATCACCAGCAGTGTACAATCATAC | $P_{eha\ w.TF}$ (amplified with CR413) |
| CR419 | GGAGAGCAGGCAAAATGTTTAGGTCTATCACACAAAAGGGATTTTTGTAATG | $P_{ehb}$ |
| CR420 | GGGGTTTCTACAGGACGTAACATATTACCACCAATCGGGACTAAAAATTTG | |
| CR421 | GGAGAGCAGGCAAAATGTTTAGTAAATCACCGTGAATTTGCGAATAATTTC | $P_{glnA}$ |
| CR422 | GGGGTTTCTACAGGACGTAACATATATATTCCTCCAAAATCATCTTTATAGGAAATAGC | |
| CR467 | GGAGAGCAGGCAAAATGTTTAGTTTATAGATTCCCGATGTTCAAATGC | $P_{fla_JJ}$ (amplified with CR244) |
| CR468 | GGAGAGCAGGCAAAATGTTTAGATTACCATCTTATTTAGCTTTATAAAAATAGTAATC | $P_{mcr_JJ}$ (amplified with CR400) |
| CR469 | GGGGTTTCTACAGGACGTAACATATTACCATCTTATTTAGCTTTATAAAAATAGTAATC | $P_{mcrR_JJ}$ (amplified with CR401) |
| CR416 | CAAAAGTGGGACTTAAGTTCCCACTTTTGCTATTGATTTATCAACATTGAGGCTTTTAGG | For suicide plasmid construction incl. homologous arms, *uidA* and vector |
| CR417 | GTGCACCAAGGATCTTCACCTAGAACTAGTGTAGATGTTCTAAAAGATAATGATTATTTAGTATTTG | |
| CR418 | GTTCCTGGCCTTTTGCTGGCCAAGCTTATTGTAAATTATGCCTCCAAGGGTG | |
| CR298 | CTAAACATTTTGCCTGCTCTCC | |
| CR415 | GGGAACTTAAGTCCCACTTTTGCTATATCTCATTGTTTGCCTCCCTGCTG | |
| SV-F | TCTAGGTGAAGATCCTTGGTGCAC | |
| SV-R | GGCCAGCAAAAGGCCAGGAAC | |
| CR426 | GTTCCTGGCCTTTTGCTGGCCAAGCTTGGATTTACCTGTTGTTATGTATTCATTTACC | ΔNrpR |
| CR427 | GTATATTACGAATAGGGCGTTTTTTATTTATAAAATGGATAAAATTTCAACATCAATATTACTGTC | |
| CR428 | GAAATTTTATCCATTTTATAAATAAAAAACGCCCTATTCGTAATATACTATTC | |
| CR429 | GGAAGGTCGTCTCCTCTAGTTTTTTTTGATATATACATCATAACATTACTCTATG | |
| CR430 | ACTAGAGGAGACGACCTTCCATGGGAAAAAAGGACAAAAGATGG | |

| | |
|---|---|
| CR431 | GTGCACCAAGGATCTTCACCTAGAACTAGTCATTTCAGTTTACGGAAAAACTGTTTC |

**Reference**


(1) Dodsworth, J. A.; Leigh, J. A. Regulation of nitrogenase by 2-oxoglutarate-reversible, direct binding of a PII-like nitrogen sensor protein to dinitrogenase. *Proc. Natl. Acad. Sci. U. S. A.* **2006**, *103* (26), 9779–9784. https://doi.org/10.1073/pnas.0602278103.

(2) Walters, A. D.; Smith, S. E.; Chong, J. P. J. Shuttle vector system for *Methanococcus maripaludis* with improved transformation efficiency. *Appl. Environ. Microbiol.* **2011**, *77* (7), 2549–2551. https://doi.org/10.1128/AEM.02919-10.

(3) Lyu, Z.; Jain, R.; Smith, P.; Fetchko, T.; Yan, Y.; Whitman, W. B. Engineering the autotroph *Methanococcus maripaludis* for geraniol production. *ACS Synth. Biol.* **2016**, *5* (7), 577–581. https://doi.org/10.1021/acssynbio.5b00267.

(4) Zetsche, B.; Gootenberg, J. S.; Abudayyeh, O. O.; Slaymaker, I. M.; Makarova, K. S.; Essletzbichler, P.; Volz, S. E.; Joung, J.; van der Oost, J.; Regev, A.; Koonin, E. V.; Zhang, F. Cpf1 Is a single RNA-guided endonuclease of a Class 2 CRISPR-Cas system. *Cell* **2015**, *163* (3), 759–771. https://doi.org/10.1016/J.CELL.2015.09.038.

(5) Ran, F. A.; Hsu, P. D.; Wright, J.; Agarwala, V.; Scott, D. A.; Zhang, F. Genome engineering using the CRISPR-Cas9 system. *Nat. Protoc.* **2013**, *8* (11), 2281–2308. https://doi.org/10.1038/nprot.2013.143.

(6) B.Whitman, W.; Shieh, J.; Sohn, S.; Caras, D. S.; Premachandran, U. Isolation and characterization of 22 mesophilic *Methanococci*. *Syst. Appl. Microbiol.* **1986**, *7* (2–3), 235–240.

(7) Fonseca, D. R.; Halim, M. F. A.; Holten, M. P.; Costa, K. C. Type IV-like pili facilitate transformation in naturally competent archaea. *J. Bacteriol.* **2020**, *202* (21), 1–12. https://doi.org/10.1128/JB.00355-20.

(8) Gibson, D. G.; Young, L.; Chuang, R. Y.; Venter, J. C.; Hutchison, C. A.; Smith, H. O. Enzymatic assembly of DNA molecules up to several hundred kilobases. *Nat. Methods* **2009**, *6* (5), 343–345. https://doi.org/10.1038/nmeth.1318.

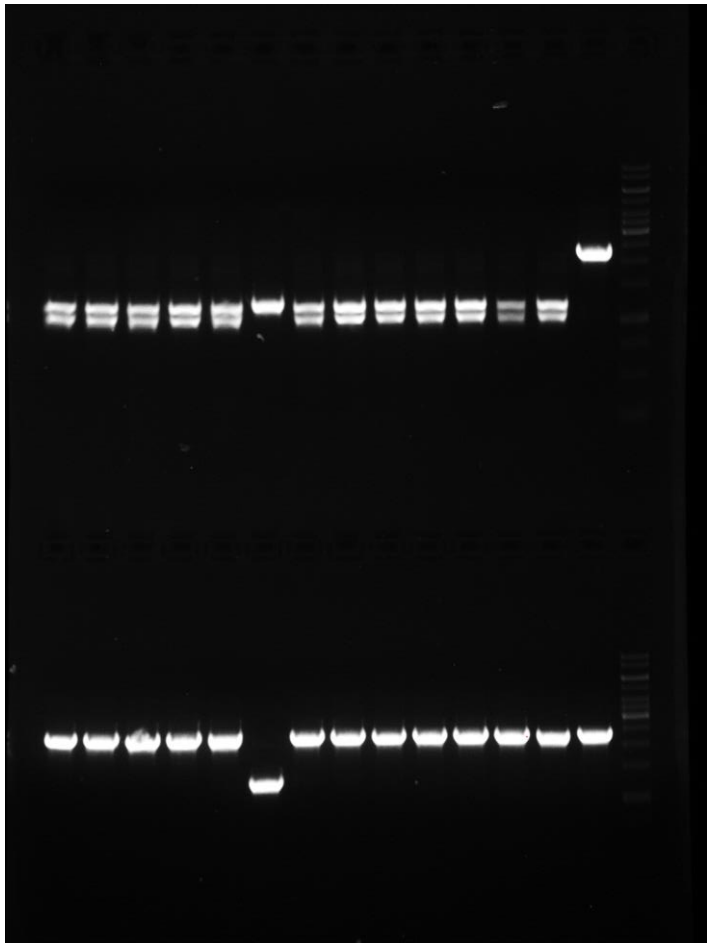

**Figure S1.** Colony PCR results for genome editing with the plasmid p002-218-L1000. Upper row: PCR products digested by NotI. Lower row: Undigested PCR products.
Lanes 1-13: individual colonies. Lane 14: wildtype. Lane 15: DNA ladder (Thermo Scientific GeneRuler 1 kb DNA ladder #SM0311). The primers amplify from 225 bp upstream and 69 bp downstream of the RF on the genome. The expected size of the PCR products of the edited transformants is 2302 bp, that of the wildtype is 2350 bp. The NotI digested PCR products (upper row) are expected to have two bands: 1227 bp and 1075 bp, if editing took place. The PCR product of the wildtype genome is not digestible by NotI.

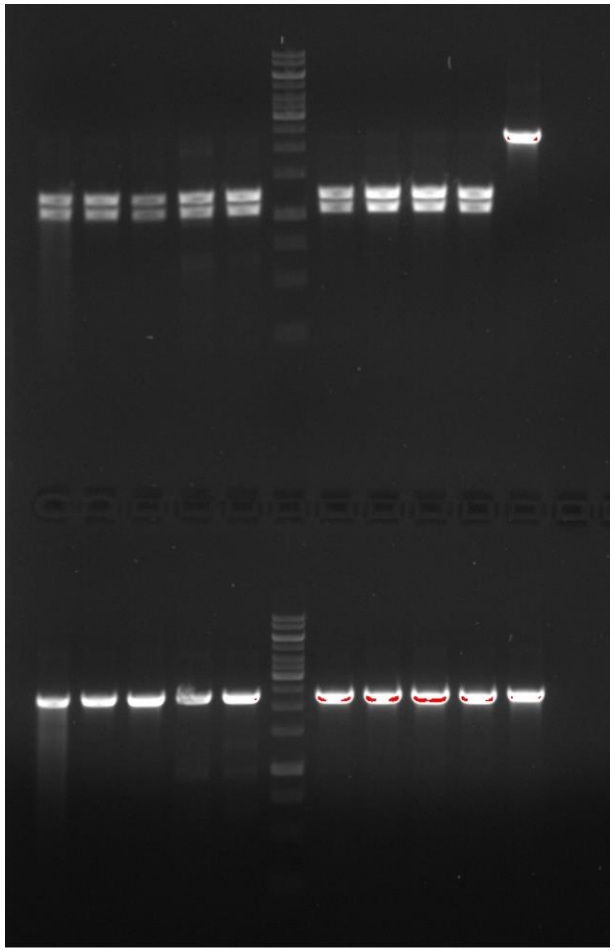

**Figure S2.** Colony PCR result of p002-218-L500 edited colonies. Upper row: PCR products digested by NotI. Lower row: Undigested PCR products.
Lanes 1-5, 7-10: individual colonies. Lane 11: wildtype. Lane 6: DNA ladder (Thermoscientific GeneRuler 1 kb DNA ladder #SM0311). The primers amplify from 725 bp upstream and 569 bp downstream of the RF on the genome. The expected size of the PCR products of the edited transformants is 2302 bp, that of the wildtype is 2350 bp. The NotI digested PCR products (upper row) are expected to have two bands: 1227 bp and 1075 bp, if editing took place. The PCR product of the wildtype genome is not digestible by NotI.

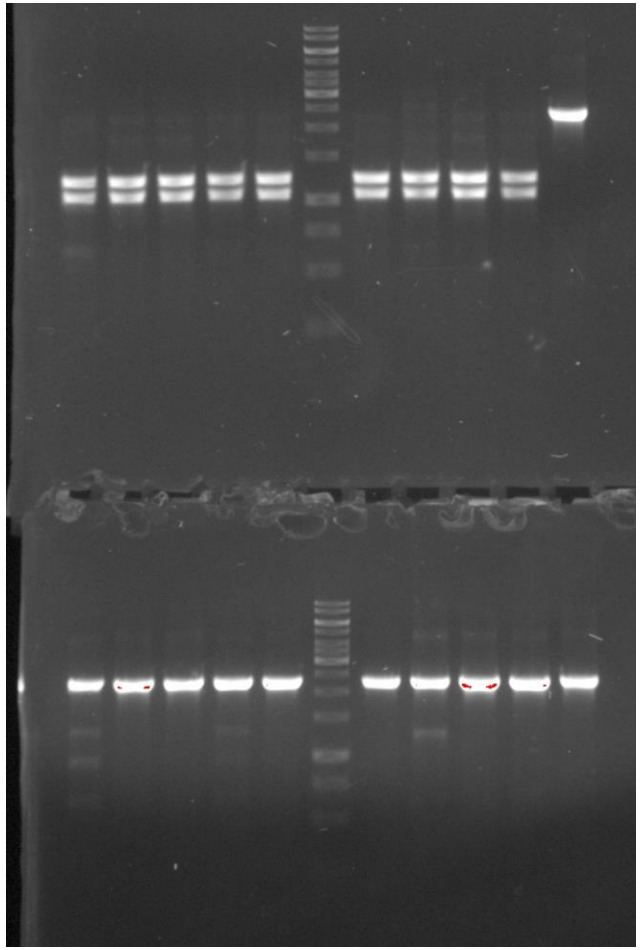

**Figure S3.** Colony PCR result of p002-218-L250 edited colonies. Upper row: PCR products digested by NotI. Lower row: Undigested PCR products.
Lanes 1-5, 7-10: individual colonies. Lane 11: wildtype. Lane 6: DNA ladder (Thermoscientific GeneRuler 1 kb DNA ladder #SM0311). The primers amplify from 725 bp upstream and 569 bp downstream of the RF on the genome. The expected size of the PCR products of the edited transformants is 2302 bp, that of the wildtype is 2350 bp. The NotI digested PCR products (upper row) are expected to have two bands: 1227 bp and 1075 bp, if editing took place. The PCR product of the wildtype genome is not digestible by NotI.

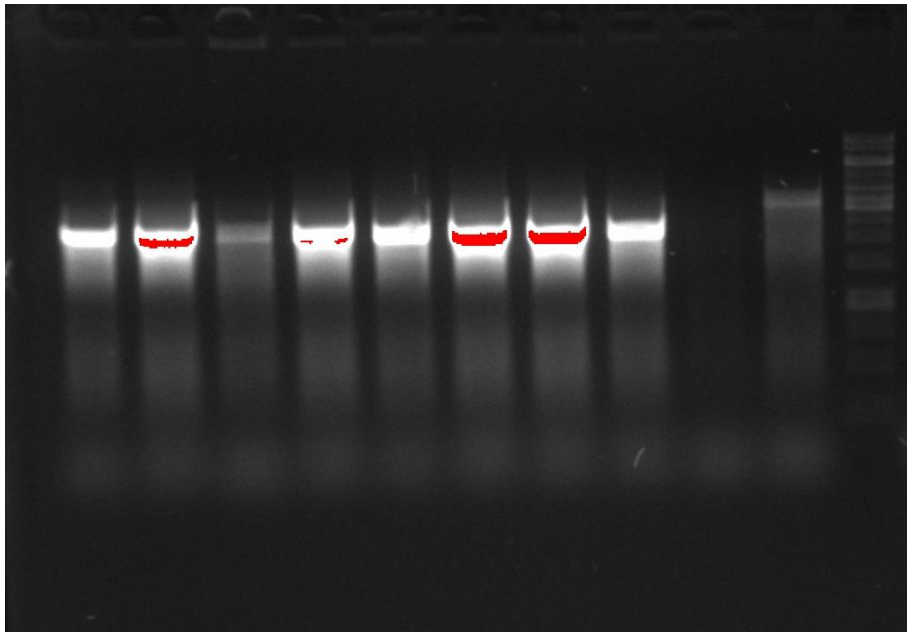

**Figure S4.** Colony PCR result of p002-218-D500 edited colonies.
Lane 1-9: individual colonies. Lane 10: wildtype. Lane 11: DNA ladder (Thermoscientific GeneRuler 1 kb DNA ladder #SM0311). The primers amplify from 215 bp upstream and 57 bp downstream of the RF on the genome. The expected size of the PCR products of the edited transformants is 2280 bp, that of the wildtype is 3274 bp.

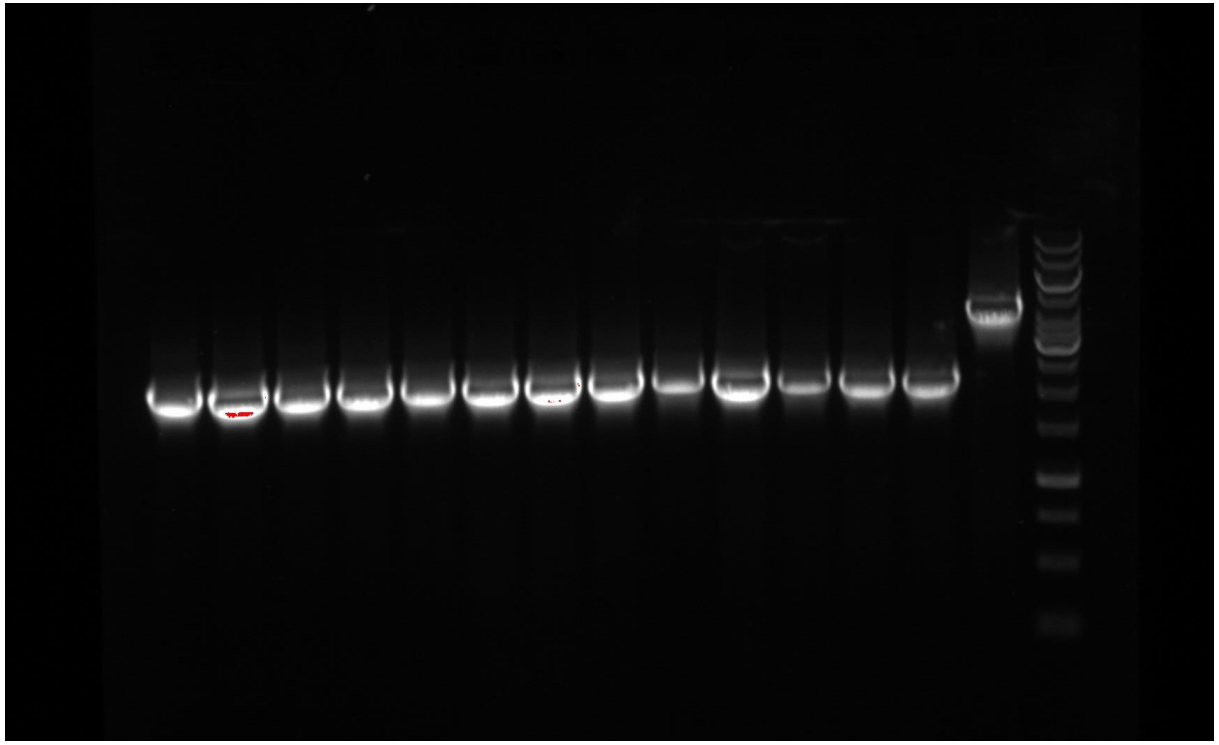

**Figure S5.** Colony PCR result of p002-218-D1000 edited colonies.
Lane 1-13: individual colonies. Lane 14: wildtype. Lane 15: DNA ladder (Thermoscientific GeneRuler 1 kb DNA ladder #SM0311). The primers amplify from 64 bp upstream and 102 bp downstream of the RF on the genome. The expected size of the PCR products of the edited transformants is 2174 bp, that of the wildtype is 4078 bp.

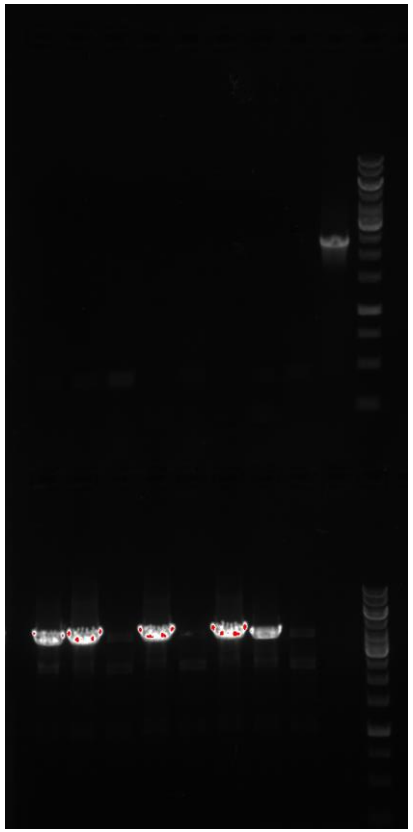

**Figure S6.** Colony PCR result of p002-218-uidA edited colonies.
Lane 1-8: individual colonies. Lane 9: wildtype. Lane 10: DNA ladder (Thermoscientific GeneRuler 1 kb DNA ladder #SM0311). Two pairs of primers were used to check whether the whole flagellum ORF were replaced with *uidA*. The upper row is the amplicon of the part of the flagellum ORF. The expected size of the amplicon of the edited transformants and wildtype genome is no band and 2350 bp, respectively. The lower row is the amplicon from 64 bp upstream and 86 bp downstream of the RF on the genome. The expected size of the PCR products of the edited transformants and wildtype genome is 3905 bp and 10983 bp, respectively. The 10983 bp band for the wildtype genome is not visible because our polymerases were not able to amplify a fragment larger than 8 kb.

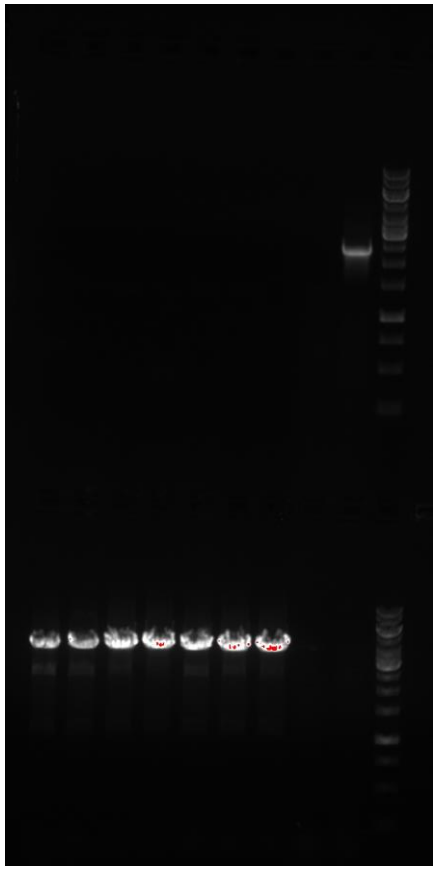

**Figure S7.** Colony PCR result of p002-226-uidA edited colonies.
Lane 1-8: individual colonies. Lane 9: wildtype. Lane 10: DNA ladder (Thermoscientific GeneRuler 1 kb DNA ladder #SM0311). Two pairs of primers were used to check whether the whole flagellum ORF were replaced with *uidA*. The upper row is the amplicon of the part of the flagellum ORF. The expected size of the amplicon of the edited transformants and wildtype genome is no band and 2350 bp, respectively. The lower row is the amplicon from 64 bp upstream and 86 bp downstream of the RF on the genome. The expected size of the PCR products of the edited transformants and wildtype genome is 3905 bp and 10983 bp, respectively. The 10983 bp band for the wildtype genome is not visible because our polymerases were not able to amplify a fragment larger than 8 kb.

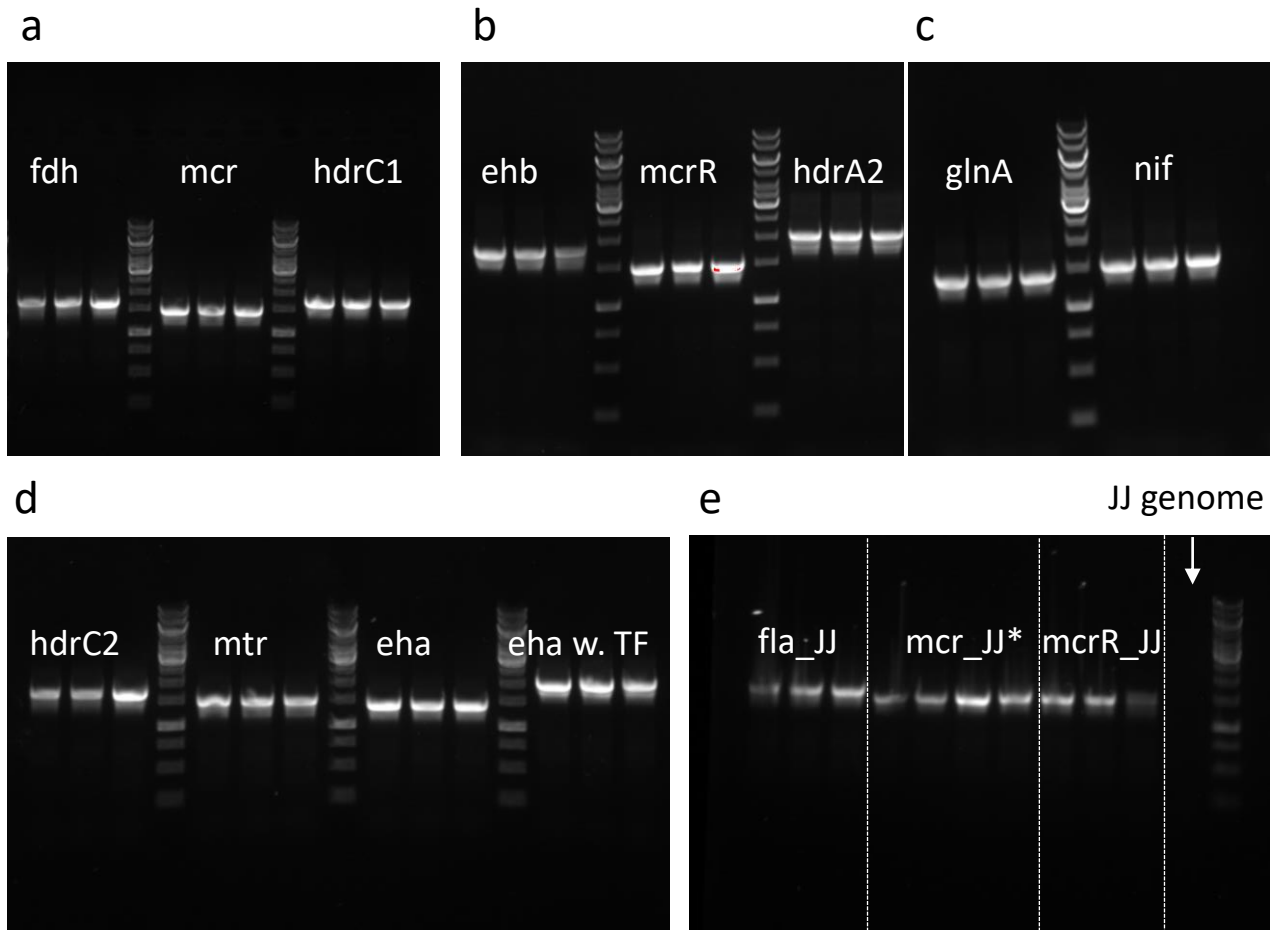


**Figure S8.** Colony PCR result of co-transforming a CRISPR/LbCas12a plasmid and a suicide plasmid with "*Promoter-uidA*" cassette flanking with 1000 bp homologous repair fragment. One pair of primers was used to check whether the "*Promoter-uidA*" cassette was successfully inserted onto the genome. The forward primer amplifies from 56 bp upstream of the up homologous arm and reverse primer amplifies from the internal of the *uidA* gene. The expected size of the amplicon of the edited transformants is 1189 bp + the size of the promoter. No band should be obtained from the wildtype genome.
*In Fig. S8e, the first mcr_JJ sample was accidentally loaded on both lanes: 4 and 5.

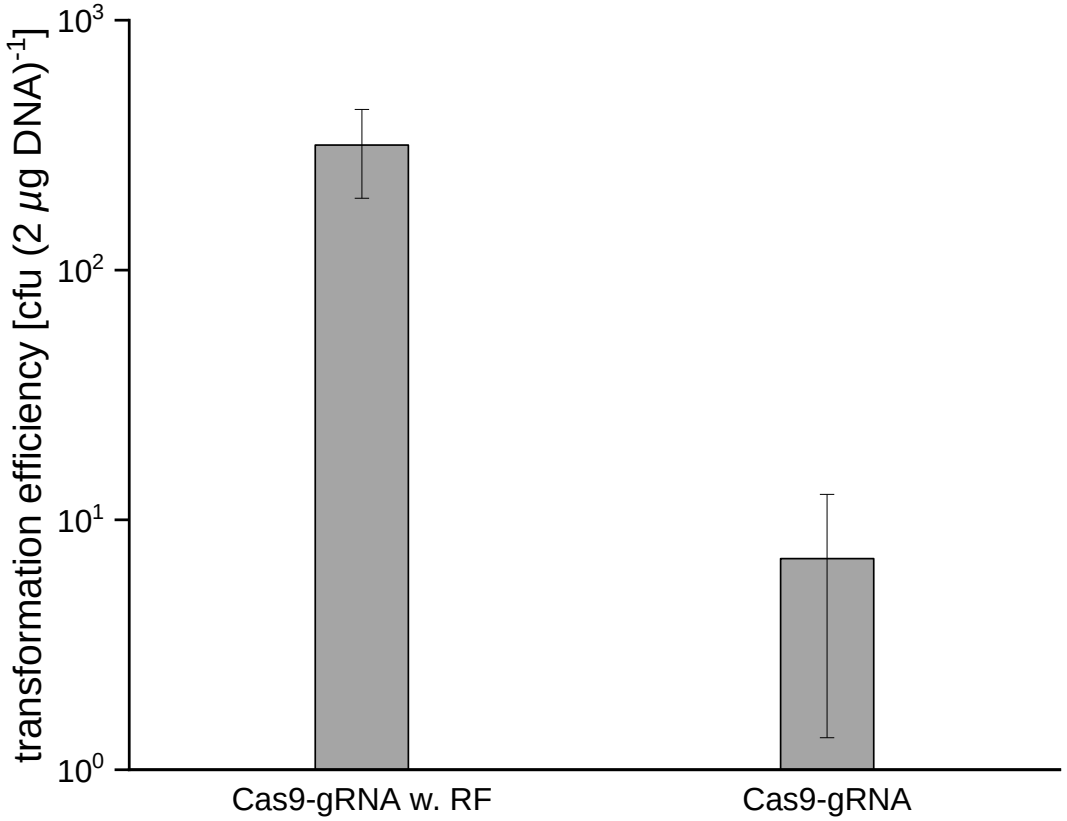


**Figure S9.** Colony forming units (cfu) for experiments using the CRISPR/Cas9 toolbox. The alanine dehydrogenase-alanine racemase (*ald-alr* 1.9 kbp) genes have been replaced by a 4.2 kbp fragment. The repair fragment (RF) has been inserted via a suicide plasmid. 2 $\mu$g of Cas9 plasmid and 2 $\mu$g of the suicide plasmid was co-transformed. The number above the bar represents the positive rate obtained via colony PCR (8 out of 10 were positive). The error bars represent the standard deviation of the biological triplicates.

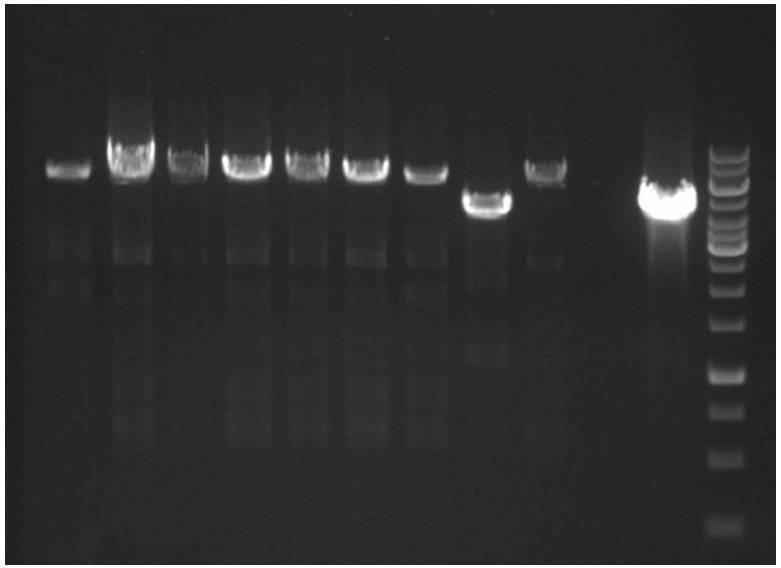

**Figure S10.** Colony PCR result of CRISPR/Cas9 toolbox edited colonies. Lane 1-10: individual colonies. Lane 11: wildtype. Lane 12: DNA ladder (Thermoscientific GeneRuler 1 kbp DNA ladder #SM0311). One pair of primers was used to check whether the *ald-alr* ORF was replaced with the 4.2 kbp fragment. The expected size of the amplicon of the edited transformants and wildtype genome is 6314 and 4367 bp, respectively.

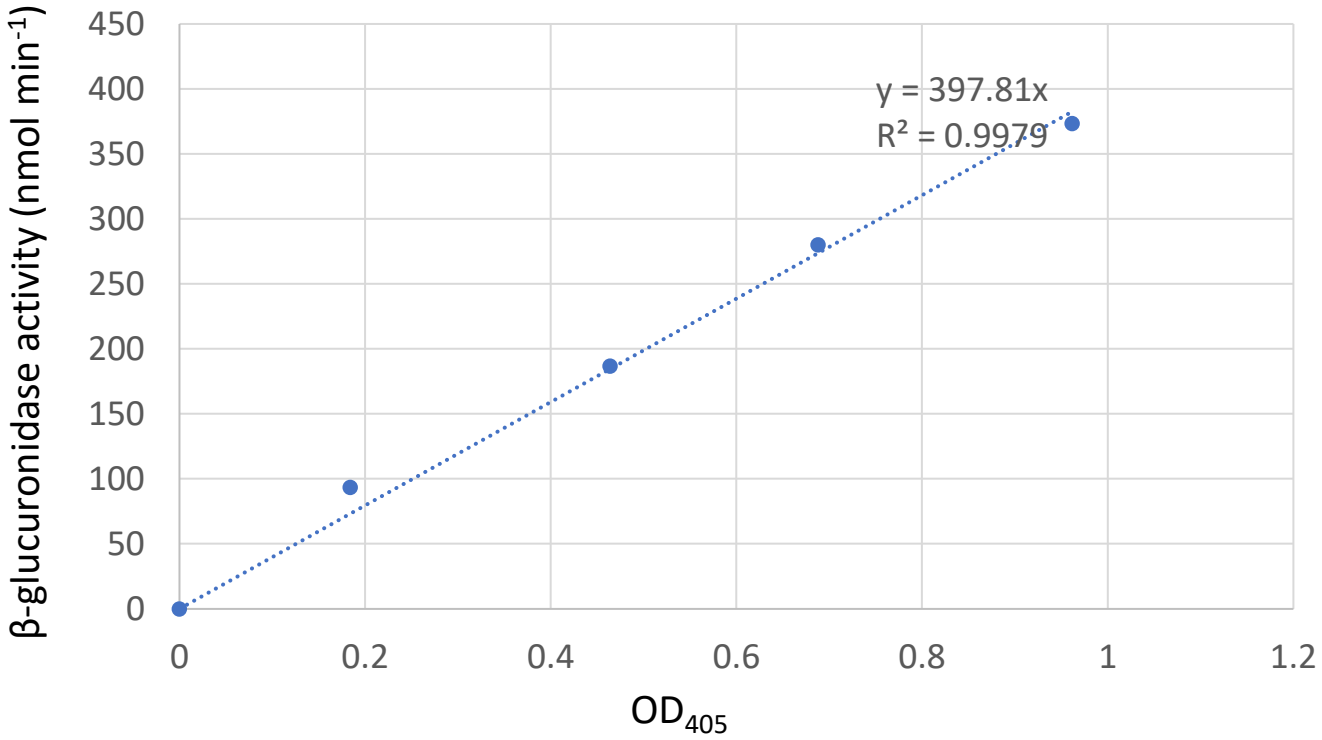


**Figure S11.** The standard curve of β-glucuronidase activity. Linear regression forcing the curve through point 0/0 yielded the conversion factor 398 nmol $min^{-1}$, that has been applied to all experiments.